

7-12-2014

Indentation vs. Uniaxial Power-law Creep of Sn-based Solder Material: A Numerical Assessment

Matthew Cordova

Follow this and additional works at: https://digitalrepository.unm.edu/me_etds

Recommended Citation

Cordova, Matthew. "Indentation vs. Uniaxial Power-law Creep of Sn-based Solder Material: A Numerical Assessment." (2014).
https://digitalrepository.unm.edu/me_etds/79

This Thesis is brought to you for free and open access by the Engineering ETDs at UNM Digital Repository. It has been accepted for inclusion in Mechanical Engineering ETDs by an authorized administrator of UNM Digital Repository. For more information, please contact disc@unm.edu.

Matthew Cordova

Candidate

Mechanical Engineering

Department

This dissertation is approved, and it is acceptable in quality and form for publication:

Approved by the Dissertation Committee:

Yu-Lin Shen , Chairperson

Mahmoud Reda Taha

Mehran Tehrani

**INDENTATION VS. UNIAXIAL POWER-LAW CREEP OF
SN-BASED SOLDER MATERIAL: A
NUMERICAL ASSESSMENT**

By

MATTHEW CORDOVA

B.S MECHANICAL, UNIVERSITY OF NEW MEXICO (2012)

THESIS

Submitted in Partial Fulfillment of the
Requirements for the Degree of

Master of Science

Mechanical Engineering

The University of New Mexico

Albuquerque, New Mexico

May 2014

Indentation vs. Uniaxial Power-law Creep of Sn-based Solder Material: A Numerical Assessment

By

MATTHEW CORDOVA

B.S. Mechanical Engineering, University of New Mexico, 2012

M.S. Mechanical Engineering, University of New Mexico, 2014

ABSTRACT

It is crucial to understand the creep behavior of Pb-free solder alloys in electronic packaging. Typical service environments are between 298 and 373K. The thermal mismatch induced stresses acting on solder joints result in extensive rate-dependent plastic deformation. The solder alloy is potentially the weakest component in the electronic package because normal operating temperatures are already above 0.5 of the melting temperature (in K). Characterization of small-volume materials has been primarily relying on the method of indentation. The topic of concern in this study is the relationship between indentation creep and uniaxial power-law creep. Two stages of numerical simulation were involved, the first a uniaxial creep test and the other an indentation test. Both were based on rate-dependent viscoplastic behavior as the input material model for the pure Sn and Sn alloys. The objective is to establish a connection between uniaxial creep and indentation creep. For conical and pyramidal indenters, the indentation strain rate is usually expressed as $\dot{\epsilon}_I = \frac{1}{h} \frac{dh}{dt}$, where h is the instantaneous indentation depth and t is time. By using this definition of indentation strain rate, the four materials studied here

were found to have stress exponents similar to the uniaxial creep response. This similar stress exponent gives rise to a near parallel strain rate-flow stress curves (on the logarithmic scale) between uniaxial creep and indentation creep. The separation between the curves thus provides the strain rate relationship between the two forms of creep. Relatively consistent ratios between uniaxial and indentation strain rates, between 0.20 to 0.28 was obtained, and can serve as guidance for obtaining uniaxial creep behavior using the indentation technique.

Table of Contents

Chapter 1	1
1. Introduction.....	1
1.1 Extraction of Creep Parameters Using Indentation.....	5
1.2 Objective of This Study.....	8
Chapter 2	9
2. Numerical Models.....	9
2.1 Background on Material Model.....	9
2.2 Simulation of Uniaxial creep Test Using Elastic-Viscoplastic Model.....	11
2.3 Simulation of Indentation Creep under Constant Strain rate.....	17
2.4 Mesh Convergence	21
Chapter 3	26
3. Uniaxial Creep Response.....	26
Chapter 4	33
4. Indentation-derived Creep Response.....	33
Chapter 5	43
5. Conclusions and Suggested Future Work.....	43
5.1 Conclusions.....	43
5.2 Suggested future studied.....	44
References	46
Appendix	48
A. Uniaxial Creep Input File For Sn @ Rate $0.0001s^{-1}$	48
B. Indentation Creep Input File For Sn @ Rate $0.0001s^{-1}$	51

List of Figures

Figure 1: Dislocation Glide-Plus-Climb.....	4
Figure 2: Constant-Load Indentation; Load vs. Depth.....	6
Figure 3: Constant Indentation Strain Rate; Load vs. Depth.....	7
Figure 4: Creep Strain vs. Time @ Constant Temperature.....	9
Figure 5: Uniaxial Model.....	13
Figure 6: Influence Of Increasing Strain Rate On Plastic Flow Stress Of Elastic-Viscoplastic Material.....	14
Figure 7: Steady-State Creep Behavior Of Sn.....	15
Figure 8: Steady-State Creep Behavior Of Sn-Ag-Cu.....	16
Figure 9: Indentation Model.....	19
Figure 10: Mesh 1.....	22
Figure 11: Mesh 2.....	23
Figure 12: Mesh 3.....	24
Figure 13: Convergence Study.....	25
Figure 14: Strain vs. Time With Material Sn-Ag-Cu.....	27
Figure 15: Viscoplastic Input Compared With Uniaxial Creep Output For Sn-Ag-Cu....	28
Figure 16: Strain vs. Time With Material Sn-Ag-Cu @ 120°C.....	28
Figure 17: Viscoplastic Input Compared With Uniaxial Creep Output For Sn-Ag-Cu @ 120°C.....	29
Figure 18: Strain vs. Time With Material Sn.....	30
Figure 19: Viscoplastic Input Compared With Uniaxial Creep Output For Sn	31
Figure 20: Strain vs. Time with Material Sn @ 120°C.....	31
Figure 21: Viscoplastic Input Compared With Uniaxial Creep Output For Sn @ 120°C...	32
Figure 22: Load vs. Depth For Sn @ Varying Strain Rate.....	34
Figure 23: Load vs. Depth For Sn @ 120°C @ Varying Strain Rate.	34

Figure 24: Load vs. Depth For Sn-Ag-Cu @ Varying Strain Rate	35
Figure 25: Load vs. Depth For Sn-Ag-Cu @ 120°C @ Varying Strain Rate.....	35
Figure 26: Equivalent Plastic Strain For Sn-Ag-Cu @ Rate $0.0001s^{-1}$	38
Figure 27: Equivalent Plastic Strain For Sn-Ag-Cu @ Rate $0.00001s^{-1}$	38
Figure 28: Equivalent Plastic Strain For Sn-Ag-Cu @ Rate $1x10^{-6}s^{-1}$	39
Figure 29: Equivalent Plastic Strain For Sn-Ag-Cu @ Rate $1x10^{-7}s^{-1}$	39
Figure 30: Von Mises Stress for Sn-Ag-Cu @ Rate $0.0001s^{-1}$	40
Figure 31: Von Mises Stress for Sn-Ag-Cu @ Rate $0.00001s^{-1}$	40
Figure 32: Von Mises Stress for Sn-Ag-Cu @ Rate $1.0x10^{-6}s^{-1}$	41
Figure 33: Von Mises Stress for Sn-Ag-Cu @ Rate $1.0x10^{-7}s^{-1}$	41
Figure 34: Steady State Strain Rate Compared With Uniaxial Strain Rate And Stress....	42

List of Tables

Table 1: Rate Dependent Yield Ratios With Corresponding Strain Rates Evaluated Through Static Plastic Stress Values Of 1.9, 1.0, 15.0, 4.0 (MPa) For Materials Sn @25°C, Sn @120°C, Sn-Ag-Cu @25°C, and Sn-Ag-Cu @ 120°C, Respective.....	14
Table 2: Material Properties Used In The finite Element Model.....	16
Table 3: 10 Loading Steps With dt Adjusted To Keep Constant $\dot{\epsilon}_I$ Of $0.0001s^{-1}$	20
Table 4: Stress Exponents For Uniaxial And Indentation Tests.....	37

Indentation vs. Uniaxial Power-law Creep of Sn-based Solder Material: A Numerical Assessment

Ch.1 Introduction

Solder in microelectronic packages serves the purpose for electric connection of the device [1-3]. Typical service environments are between 298 and 373K. The thermal mismatch induced stresses acting on solder joints result in extensive rate-dependent plastic deformation. The solder joint is potentially the weakest component in the electronic packages because normal operating temperatures are already above 0.5 of the melting temperature (in K) [2,4-7]. Within recent years traditional tin (Sn)-lead (Pb) solder alloy, because of the harm to the environment it induces, has attracted worldwide attention to move towards Pb-free solders [1,2,4,6-9]. The European Union has mandated a ban on the use of lead in electronic products that began in mid-2006 [9]. Due to the widespread use of lead in manufacturing and assembly of circuit boards the need to develop a reliable Pb-free solder is crucial for the substitution with Sn-based materials. Currently Sn-based alloys constitute the dominant Pb-free solder material. It is necessary to understand the mechanical behavior of the solder alloy for dependability of the electronic devices.

Characterization of small scaled materials plays an important role in reliability assessment of electronic packaging and is critical in package design and manufacturing [1,3]. The indentation method has been generally used to study mechanical properties and deformation behavior in small volumes of materials, and to understand their rate-dependent processes such as creep [5,10-12]. Understanding the mechanical behavior of solder alloys is extremely important, because they must perform under challenging thermo-mechanical conditions such as creep, thermo-mechanical fatigue, vibration,

mechanical shock, and thermal aging [9,13]. Creep resistance of solder material is important, since room temperature is already high enough to induce time-dependent deformation. The reliability in microelectronic packaging depends on time-dependent deformation and the associated failure mechanisms.

Creep of Sn-rich alloys can be classified into two groups: bulk alloy behavior and solder joint level. Creep behavior is directly related to the microstructure, which is a strong function of cooling rate during processing. A smaller joint (< 1 mm) have a finer and more repetitive microstructure than larger bulk specimens which have a somewhat coarser microstructure [7,9]. Furthermore, bulk solder samples usually display considerable spatial variations in microstructure due to differences in local solidification rate [7,8]. Significant research has been focused on mechanical properties of bulk lead-free solder alloys; however, fewer studies have been done on small-scale experimental characterization of solder joints [1].

The nanoindentation technique is widely used to characterize mechanical properties of small-scale structure without destruction of the sample. Multiple indentation tests can even be performed on the same sample. This technique also provides accurate controls on load, displacement and position that, if known, can give a great deal of information about mechanical properties and deformation of the material [1,3,11,13,14]. The measurement of time-dependent phenomena can be divided into two classes, broadband quasistatic, or creep techniques where the load, stress or strain rate is held constant for a specific time while the material is measured. The other technique is frequency-specific dynamic, where the load or stress is carried at a single frequency and the response of the material is measured [13]. Standard bulk-testing exists for these

techniques, but these techniques become impractical if the volume of material of interest is on a small scale [13].

There are several differences between indentation and conventional creep testing. Conventional creep tests have either constant uniaxial stress or constant strain rate (usually less than $10^{-4} s^{-1}$). In uniaxial testing the geometry of the specimen is usually a simple one; a dog bone tensile test or a cylindrical compression test are common. When performing an indentation test, the geometry of the test is being controlled by the very properties of the material that are of interest, for example hardness, Young's modulus, and strain rate sensitivity. The tests are specifically designed to extract the properties of interest [13,22].

For small-scale materials such as solder alloys, it is difficult to conduct bulk tests. Although indentation testing is an efficient way to acquire strain rate sensitivity of materials, the comparison of the results of indentation test and uniaxial creep is often the most concerned [1]. In an indentation test, the dynamics of deformation are different from a conventional uniaxial creep test. The stress and deformation fields are complex under indentation, so correlating the indentation measurement with uniaxial creep behavior becomes a challenge. The deformed volume of material under the indenter is constantly expanding to incorporate previously undeformed material. The creep process is believed to depend upon rate at which the elastic/plastic boundary can proceed into the material [13,15]. During a typical creep test using a bulk specimen, a constant uniaxial stress or load is applied and the deformation of material is measured as a function of time. The variation of strain as a function of time will reach the secondary or constant rate stage. The time rate of strain is then known as the steady-state strain rate $\dot{\epsilon}_s$ [16].

Most crystalline materials at temperatures above $0.5 T_m$ (with T_m being the melting point in K) show time-dependent deformation mechanisms, such as dislocation glide-plus-climb which is well described by power-law creep [16]. Dislocation glide-plus-climb can be observed in Figure 1 where dislocations will glide along a slip plane until an obstacle obstructs its movement; then another dislocation mechanism will allow the dislocation to climb to another slip plane. This glide-plus-climb development will continue at a steady state which is best described by power-law creep. A simplified steady-state creep rate equation is shown for a constant temperature,

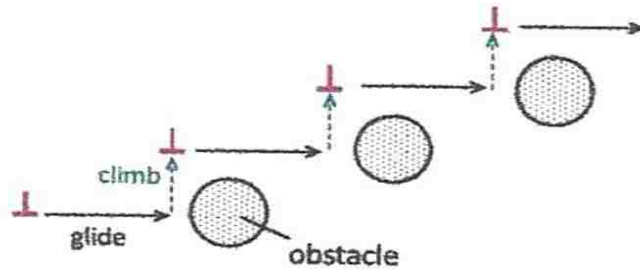


Figure 1: Dislocation glide-plus-climb [16]

$$\dot{\epsilon}_s = A\sigma^{n_c}, \quad (1)$$

where A represents a temperature-dependent material constant, σ a fixed applied stress, and n_c the stress exponent. Note that the current study focuses on creep response at constant temperatures, so the temperature dependence dictated by the activation energy is not explicitly expressed in Eq.(1). For conventional uniaxial creep tests, the constant A and stress exponent n_c can be uniquely determined by plotting the measured steady-state rates against the respective applied stresses. The main issue concerning indentation

creep tests is then to establish a procedure so the same creep parameters can be reliably obtained. In the following section, the current state of knowledge of indentation creep measurement is briefly reviewed.

1.1 Extraction of creep parameters using indentation

Traditionally there are primarily four types of depth-sensing indentation approaches used to gain insight between indentation strain rate and hardness. Indentation load relaxation tests, constant rate of loading tests, constant-load indentation creep test, and impression creep tests. All tests have drawn similarities between hardness and flow strength [13]. Since flow stress of a material is a function of strain rate and temperature, the hardness of a material must be expected to vary in a comparable way [12,13]. The relationship between hardness and flow stress is also needed in this study and will be presented in the following chapter. In addition to the traditional approaches the numerical tests in this thesis will be conducted using the constant target indentation strain rate technique along with a conical indenter. This technique allows us to provide a target constant strain rate to a desired depth that is dependent on the shape of the indenter. During indentation, the most appropriate definition of “indentation strain rate” is the instantaneous change in contact area divided by the instantaneous contact area, which is equivalent to $\frac{\dot{h}}{h}$, with h being the instantaneous indentation depth, for geometrically self-similar indenter shape [6]. Once the desired depth is reached the hardness value can be extracted to find useful parameters of the material. Other techniques are also useful such as constant-load indentation creep tests shown in Figure 2; however, there is no ability to control the rate at which the indenter penetrates the sample [13]. Another issue with this

test is that the depth of the indenter will continue to deform into the material which makes it difficult to calculate the hardness value as it will continue to decrease over time [13]. The constant strain rate technique shown in Figure 3 is used in the present study. This technique gives the ability to control the issues that a constant-load indentation test creates, and has been applied experimentally to show that it can closely approximate the steady-state creep condition [11,13,17]. Knowing the rate of indentation is significant as it will be used to relate indentation strain rate and uniaxial strain rate, which is the basis of this study.

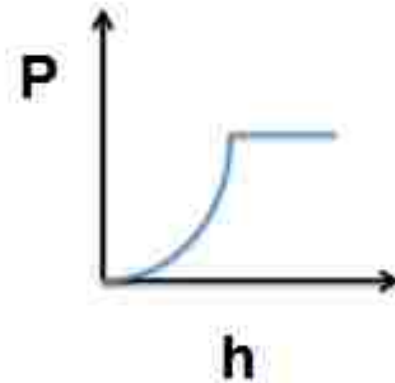


Figure 2: Constant-load indentation; load vs. depth

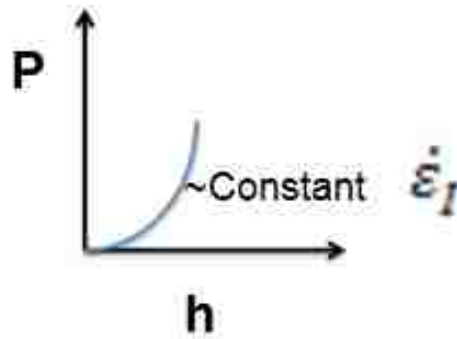


Figure 3: Constant indentation strain rate; load vs. depth

Note that the determination of stress exponent n_c is relatively straightforward, and it has been shown that indentation creep tests give rise to approximately the same stress exponent values as obtained from uniaxial creep tests [1,10,13,17,18]. The main difficulty in correlating indentation creep and conventional uniaxial creep is then the determination of constant A in Eq.(1), which requires the quantitative relationship between indentation strain rate and uniaxial strain rate. There is yet to be an accepted or validated method for such correlation [14]. The only attempt to date is by Poisl et al.[14], for an experimental characterization of amorphous selenium (Se) which is essentially a Newtonian fluid at above its glass transition temperature. They found that the ratio of uniaxial strain rate and indentation strain rate during creep is about 0.09, for this unique material with a stress exponent of unity. This result cannot be applied to other metallic material with a power-law creep response (with $n_c \neq 1$). The correlation between indentation strain rate and uniaxial strain rate under the power-law creep condition has not been established [10].

1.2 Objectives of this study

This thesis objective is to use the numerical finite element modeling technique to correlate the indentation strain rate with that of uniaxial strain rate for the power-law creep materials considered. In so doing we also illustrate numerically that the indentation creep test will yield approximately the same stress exponent as in the uniaxial creep test. Attention is devoted to the metal tin (Sn) and Sn-based solder alloys, all of which display the power-law creep behavior even at room temperature. The numerical finding will thus provide quantitative guidance on how to extract the uniaxial creep parameters from the constant strain rate indentation creep test.

When performing finite element analyses of indentation testing, a simple power-law creep material model will lead to a very stiff response which does not resemble the actual measurement. Therefore, we adopt a viscoplastic approach in the simulation to account for the rate-dependent process. As a consequence, there is a need to first demonstrate the validity of the current approach in representing the creep response. Modeling of constant-load uniaxial creep using the viscoplastic input property was thus undertaken first, to prove that the steady-state creep output can be obtained with great consistency. This same viscoplastic input was then applied to the indentation modeling to represent the creeping material. Details of the present two-stage analysis process are given in Chapter 2.

Ch.2 Numerical Models

2.1 Background on material model

Under a fixed uniaxial applied stress, there are three stages of creep that can be experienced by the specimen. The first stage is primary creep which is dominated by strain hardening and starts immediately after ϵ_0 , or instantaneous strain caused by the applied load [16]. This stage is relatively short in comparison to the total strain-time curve. The second stage, “steady state” creep, represents a dynamic balance between hardening and softening. At this state the strain rate $\frac{d\epsilon}{dt}$ is constant. The third stage is also referred to as tertiary creep, which displays an increase in $\frac{d\epsilon}{dt}$. At this stage necking, microcracking, and/or microvoid formation will start to occur till rupture [16]. The three stages of creep can be shown in Figure 4.

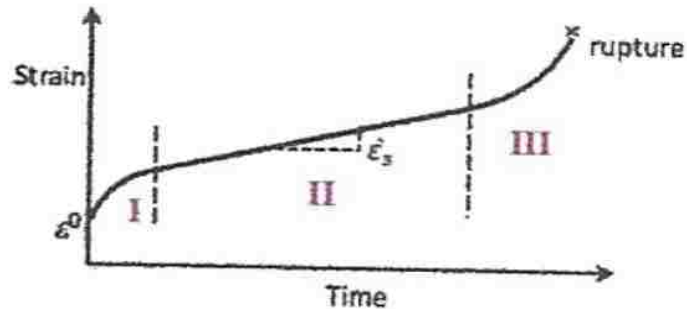


Figure 4: Creep strain vs. time at constant temperature [16]

A commonly used technique to quantify the time-dependent deformation behavior is the uniaxial constant-stress creep test. After a steady state is reached where

the strain rate remains close to constant, the relationship between strain rate, applied stress, and temperature can be expressed as [19].

$$\dot{\epsilon}_s = A' \cdot \sigma^{n_c} \cdot e^{-\frac{Q}{RT}}, \quad (2)$$

where A' is a constant, σ is the applied stress, n_c is the stress exponent for creep, Q is the activation energy, R is the universal gas constant (8.314 J/mol K), and T is the absolute temperature. Note that in this equation $A' \cdot e^{-\frac{Q}{RT}}$ is equivalent to the constant A in Eq.(1).

Viscoplasticity is a theory that describes the rate-dependent inelastic behavior of solids existent in alloys, amorphous (non-crystalline) polymer and glasses in a certain temperature range. When mechanical loading occurs at elevated temperatures or, for low-melting-point materials even at room temperature, deformation may become a function of time [19]. Time dependence can also be established using the method that material strength is a function of strain rate, not just strain [12,16]. A material will become stronger when a faster strain rate is applied. Equation 3 represents a simple viscoplastic model which is based on the static stress-strain relation, with a parameter to quantify the strain rate hardening effect [16],

$$\sigma_e = h(\int d\bar{\epsilon}^p) \cdot R \left(\frac{d\bar{\epsilon}^p}{dt} \right), \quad (3)$$

where σ_e is the von Mises effective stress, h (as a function of plastic strain $\int d\bar{\epsilon}^p$) is the static plastic stress-strain response, and R , a function of plastic strain rate $\frac{d\bar{\epsilon}^p}{dt}$, defines the ratio of flow stress at non-zero strain rate to the static plastic flow stress (where $R=1.0$). A frequent expression to relate viscoplastic stress and strain rate is.

$$\sigma = D\dot{\varepsilon}^m, \quad (4)$$

where D is a constant that incorporates the $\sigma - \varepsilon$ shape, $\dot{\varepsilon}$ is the time rate of strain and m is a material parameter also known as strain rate sensitivity factor.

As described in Chapter 1, a main purpose of this study is to establish a connection between viscoplasticity and the commonly conceived creep deformation, through numerical illustrations. The material system of interest is tin (Sn) and its alloys, which display time-dependent plastic behavior even at room temperature. Since plasticity-based models are easily implemented and widely used in indentation modeling, the viscoplasticity approach is thus chosen to describe the time-dependent deformation in this study. Therefore, there is a need to first make sure that the viscoplastic model can indeed give rise to a typical uniaxial creep response.

2.2 Simulation of uniaxial creep test using elastic-viscoplastic model

In this section we describe the numerical finite element model. All the analysis was done in ABAQUS 6.12-1. The main objective here is to illustrate that steady-state creep response can be established by using the viscoplasticity approach.

The computational model is shown in Figure 5. This model represents a cylindrical specimen with radius $1\mu m$ and height of $1\mu m$. Since this test is uniaxial and axially symmetric, only a two-dimensional domain is needed to create an accurate model. Although a single element is sufficient for the uniform loading, a total of 16 elements with 25 nodes are still used for constructing the model. The elements used in this study are of type CAX4 in Abaqus, representing “continuum axisymmetric 4 node quadrilateral elements” [20]. When assigning the applied force to act on a node the *Equation

command was used in Abaqus (see the complete input file in Appendix A for details). This command allows the user to define linear multi-point constraints in the model. This model uses these constraints and ties them to the top boundary nodes. Using an assigned node set and a degree of freedom in the y-direction, the top nodes are thus able to move together and simulates an equal uniform pulling force when a force is assigned to a user defined master node.

The y-direction in Figure 5 represents the loading direction; the x-direction represents the radius direction. The boundary conditions for this uniaxial creep model consist of fixing the bottom nodes and only allowing them to move in the x-direction similar to a roller constrain to the bottom edge. This allows the diameter to shrink after the load is applied. The left boundary of the model which simulates the center symmetry axis of the bar, is fixed in the x-direction and free in the y-direction. This allows the bar to deform along loading axis and is also similar to a roller constrain.

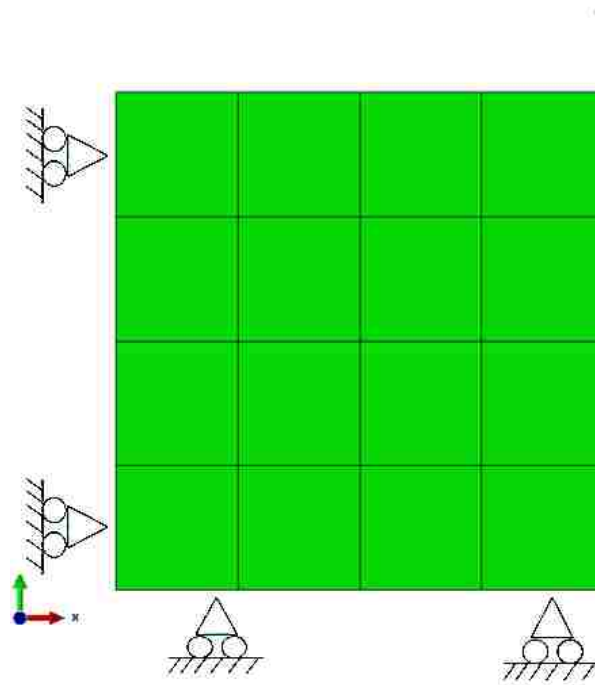


Figure 5: Uniaxial Model

This simulation assumes elastic-perfectly plastic response for four model materials. Rate dependent yield behavior is included in the model to simulate and define a material's rate dependent yield strength [20]. Figure 6 displays the influence of applied strain rate on plastic flow stress of an elastic-viscoplastic material. The rate dependent yield behavior is implemented by defining the yield ratios R at different strain rates. Table 1 displays the yield ratios and the static plastic flow stress for Sn @ 25°C with its corresponding strain rates. The steady state $\dot{\epsilon}_s$ values are found using Eq.(1) with the A and n_c constants in Table 2 where σ from Eq.(1) is the stress at a non-zero strain rate.





Sn @25°C		Sn @120°C		Sn-Ag-Cu @25°C		Sn-Ag-Cu @120°C	
Yield Ratio	Strain Rate 	Yield Ratio	Strain Rate 	Yield Ratio	Strain Rate 	Yield Ratio	Strain Rate 
1.00	0	1.00	0	1.00	0	1.00	0
1.00	1.11E-10	1.00	1.22E-09	1.00	1.12E-10	1.00	4.91E-12
1.05	1.58E-10	2.00	1.56E-07	1.20	6.96E-10	1.25	2.93E-11
1.11	2.23E-10	3.00	2.67E-06	1.33	2.00E-09	1.50	1.26E-10
2.11	2.03E-08	4.00	2.00E-05	1.67	1.86E-08	2.00	1.26E-09
3.16	3.47E-07	5.00	9.53E-05	2.00	1.15E-07	2.50	7.49E-09
4.21	2.60E-06	6.00	3.42E-04	2.13	2.19E-07	3.75	1.92E-07
4.74	5.92E-06	8.00	2.56E-03	2.53	1.22E-06	4.75	1.27E-06
5.79	2.41E-05	9.00	5.84E-03	2.67	2.04E-06	5.25	2.83E-06
7.37	1.31E-04			2.80	3.33E-06	7.50	4.92E-05
				3.33	1.90E-05	8.25	1.05E-04

Table 1: Rate dependent yield ratios with corresponding strain rates evaluated

through static plastic stress values of 1.9, 1.0, 15.0, 4.0 (MPa) for materials

Sn @25°C, Sn @120°C, Sn-Ag-Cu @25°C, and Sn-Ag-Cu @ 120°C, respectively

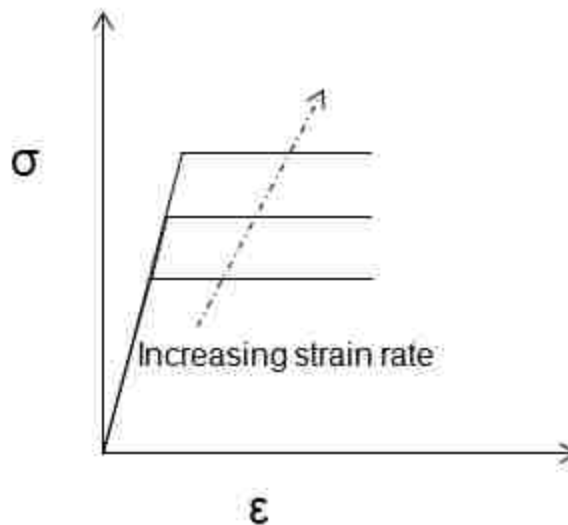


Figure 6: Influence of increasing strain rate on plastic flow stress of elastic-viscoplastic material

Steady-state creep rates as a function of stress were extracted from the published experimental results in Figures 7-8 and used as the input for the yield stress ratios [9]. The steady state creep results included materials of Sn at 25°C and 120°C(Fig.7), and also Sn-Ag-Cu alloy at 25°C and 120°C (Fig.8). For each of these curves the creep exponent n_c , which is labeled in Figures 7 and 8, is used to calculate the constant A in the simplified power-law creep equation for the respective constant temperature (see Equation 1). Table 2 displays the input material properties used for this finite element model.

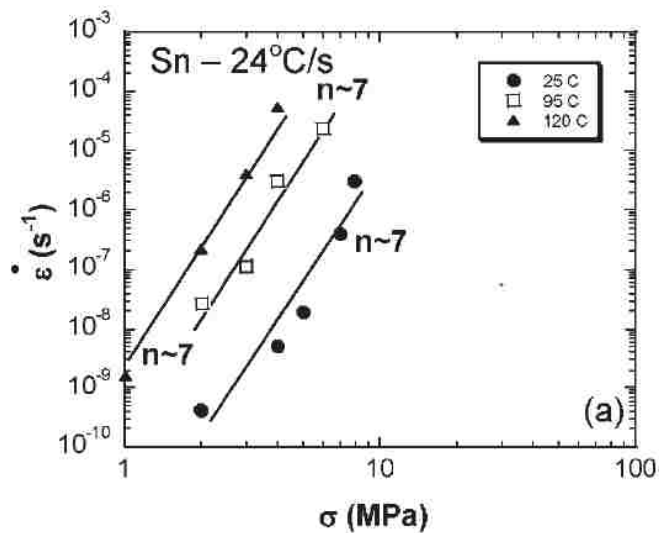


Figure 7: Steady-state creep behavior of Sn [9]

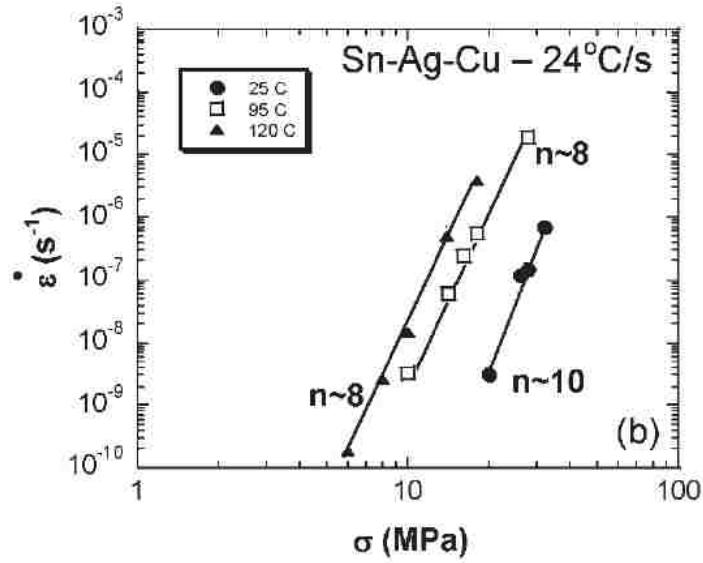


Figure 8: Steady-state creep behavior of Sn-Ag-Cu [9]

Material	Young's Modulus (MPa)	Static Plastic Flow Stress (MPa)	Poisson's ratio	$A(\text{MPa})^{-n_c} \text{s}^{-1}$	n_c
Sn-Ag-Cu @25°C	52000	15	0.35	1.95E-22	10
Sn @25°C	46000	1.9	0.28	1.24E-12	7
Sn-Ag-Cu @120°C	52000	4	0.35	7.49E-17	8
Sn @120°C	46000	1	0.28	1.22E-09	7

Table 2: Material properties used in the finite element model (The constants A and n_c were not directly used in the model. Rather, they are used for determining the yield ratio for the input viscoplastic behavior.

The loading process involves two steps. First, a total load is quickly applied within 0.01 s to achieve the desired uniaxial stress. The constant load is then maintained for a time of 30 s, during which the material will continue to deform. A linear response of strain vs. time during this hold step will indicate that steady-state creep is reached. The steady state creep rate can then be extracted and compared with the input viscoplastic parameters (i.e., the correspondence between strain rate and applied stress), to confirm that the viscoplastic model indeed leads to the conventional uniaxial creep behavior. The results will be presented in chapter 3.

2.3 Simulation of indentation creep under constant strain rate

In this section we provide details on the numerical model for the indentation creep simulation. The same modeling software, ABAQUS6.12-1, is used. This finite element model frame work has been validated and extensively applied to similar indentation analysis [19].

The modeling sample to be indented is a cylindrical homogeneous material with radius 200 μm and height 200 μm . Conical indenters have an advantage of possessing axial symmetry. The indenter portion to be in contact with the material is based on the equal projected cross-sectional area of contact between conical and pyramidal indenters. The equivalent cone semi-angle for a Berkovich indenter is 70.29°[18].

A total of 61608 continuum axisymmetric 4-node quadrilateral elements are used. A bias in mesh was implemented to align the nodes closer to the indenter zone where the highest stresses and deformation will take place. A bias was also created and assigned to the indenter; the nodes in the indenter are aligned closer together where contact with the

sample will be made. To simulate the contact between the indenter and sample, a surface command option is implemented to define surfaces for contact. Then a contact pair command is used to define the pairs of surfaces that may be contacted (see Appendix B for details). Given that contact is being made between a diamond and a metallic material, a coefficient of friction of 0.1 is used to define the surface interaction [21].

Figure 9 displays the indentation model. The left boundary (which is the symmetry axis) is only allowed to move in the y-direction and is fixed in the x-direction. The bottom boundary is fixed in the y-direction and free in the x-direction. The indenters left boundary is also fixed in the x-direction and allowed to move in the y-direction. As in the uniaxial test this simulation assumes an elastic-perfectly plastic response for the same four materials. Rate-dependent yield behavior is included in the model as described in Section 2.2. The material properties are the same as in Table 2. The Young's modulus and Poisson ratio of the diamond indenter are, respectively, 1141 GPa and 0.07 [19].

When applying the loading, the top boundary nodes of the indenter are constrained to have the same displacement in the y-direction. By adjusting the time rate of the displacement, different indentation rates can be prescribed.

The numerical model employed in Section 2.2 is intended to demonstrate that steady-state creep response can be established by simply using the viscoplasticity approach. The present indentation analysis is thus to utilize the viscoplasticity model to represent the creeping material, and explore the relationship between uniaxial creep and indentation creep. For conical and pyramidal indenters, the indentation strain rate is usually expressed as [10,13,14,17,18].

$$\dot{\epsilon}_I = \frac{1}{h} \frac{dh}{dt}, \quad (5)$$

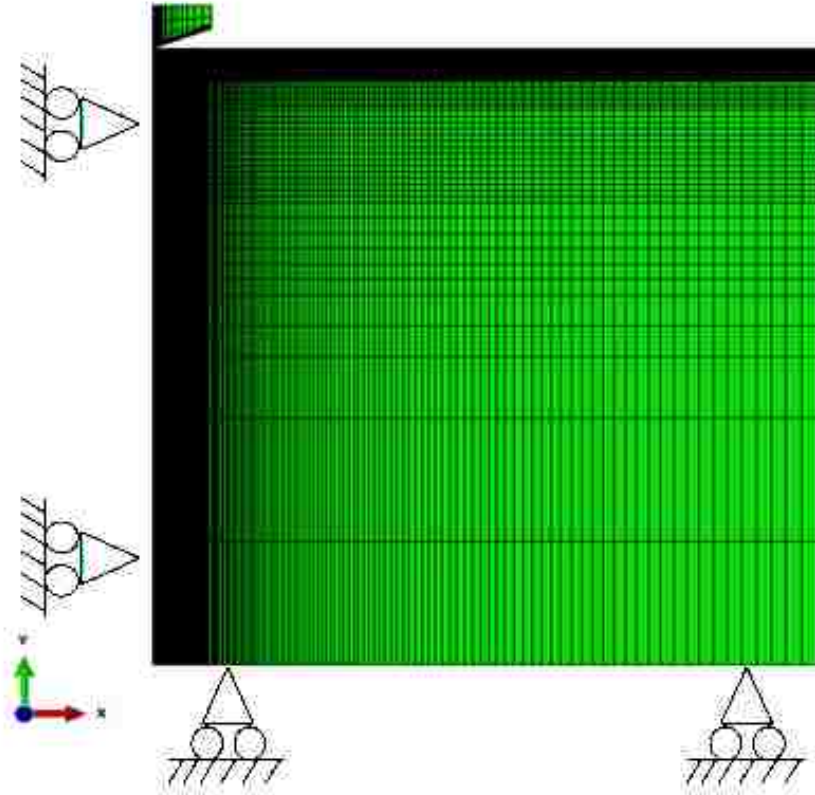


Figure 9: Indentation Model

where h is the displacement at a given time and \dot{h} is the velocity of the indenter. Imposing a constant $\dot{\epsilon}_I$ during indentation is then equivalent to a constant strain rate test. It should be noted that, in an indentation test, the strain field is non-uniform so Eq.(5) represents the “indentation strain rate” in an average sense and has been shown to be a reasonable representative strain rate in describing creep response of materials [10,13,14,17,18]. In the present indentation modeling the constant strain rate is implemented in a piecewise manner over 10 loading steps. In each step the time duration

(dt) is adjusted to keep a desired constant $\dot{\epsilon}_I$ for the entire indentation history in an approximate manner (see table 3). Throughout this indentation model four target indentation strain rates were selected $1 \times 10^{-4} \text{s}^{-1}$, $1 \times 10^{-5} \text{s}^{-1}$, $1 \times 10^{-6} \text{s}^{-1}$, and $1 \times 10^{-7} \text{s}^{-1}$.

Steps	h	dh	dt
1	0.4	0.4	10000
2	0.8	0.4	5000
3	1.2	0.4	3333
4	1.6	0.4	2500
5	2	0.4	2000
6	2.4	0.4	1666
7	2.8	0.4	1428
8	3.2	0.4	1250
9	3.6	0.4	1111
10	4	0.4	1000

Table 3: 10 loading steps with dt adjusted to keep constant $\dot{\epsilon}_I$ of 0.0001s^{-1}

In order to obtain the correspondence between indentation creep and uniaxial creep, the relationship between hardness and stress, and between indentation strain rate and uniaxial strain rate must be known. The hardness is defined as the instantaneous load P divided by the projected contact area A_c .

$$H = \frac{P}{A_c}, \quad (6)$$

where

$$A_c = \pi a^2, \quad (7)$$

with a being the radius at the contact edge. In this work P is obtained at the maximum indentation depth of $4 \mu\text{m}$. The hardness values at the various indentation strain rates are then divided by 3[23],

$$\sigma_F = \frac{H}{3}, \quad (8)$$

to obtain the corresponding plastic flow stresses σ_F resulting from indentation. This indentation strain rate-flow stress relation can then be compared with the uniaxial strain rate-flow stress relation (the model input). The difference between uniaxial strain rate and indentation strain rate can therefore be quantified.

2.4 Mesh Convergence

To justify that this model has an adequate density of nodes and elements, several mesh geometries were constructed to check for convergence. Specifically, three types of mesh, with different elements densities around the indentation zone, were constructed. The first trial is shown in Figure 10: Mesh 1 has a uniform zone of dimension $25 \times 25 \mu m$ around the area of indentation. In this area there are a total of 9801 elements (99 by 99). Beyond the uniform square holds no importance for a dense mesh, therefore the elements are no longer needed to be uniform and can be spaced further apart to comprise a more computationally friendly model.

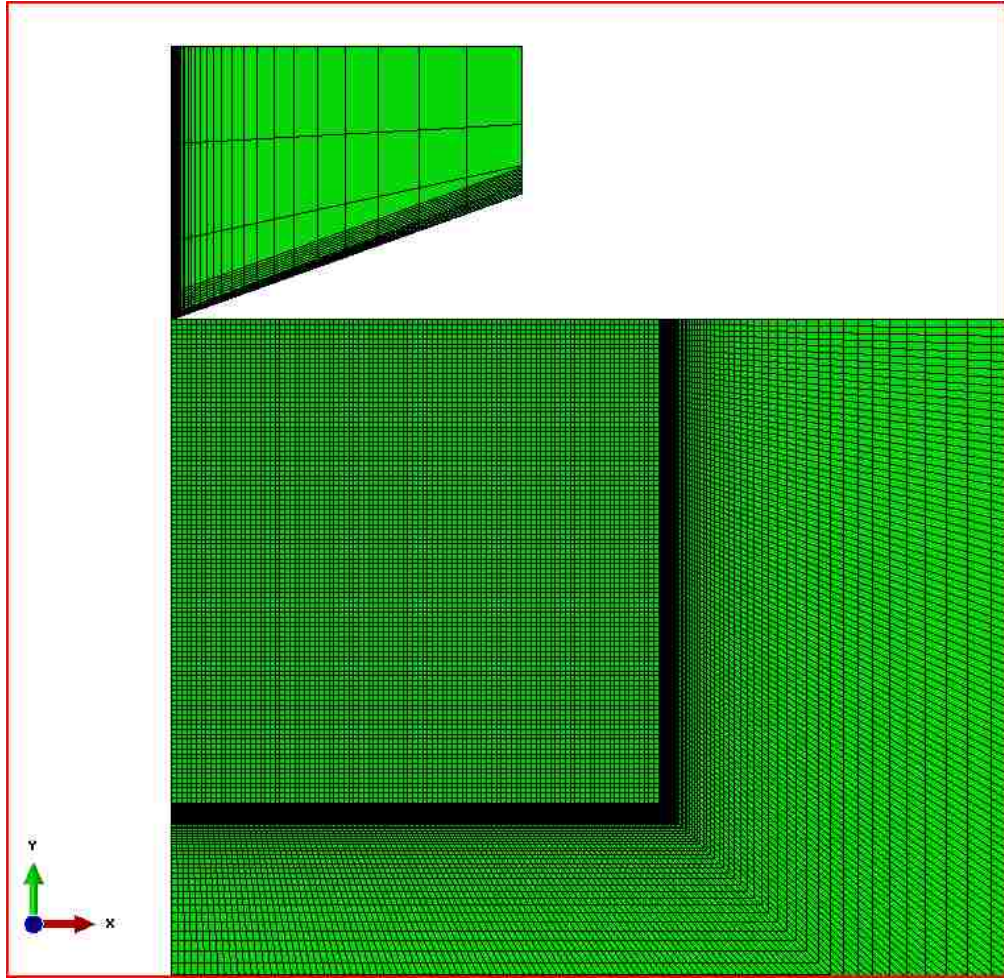


Figure 10: Mesh 1

Mesh 2 is very similar to the first, however with a much higher 39691 elements (199 by 199) in the same zone of $25 \times 25 \mu m$, as shown in Figure 11.

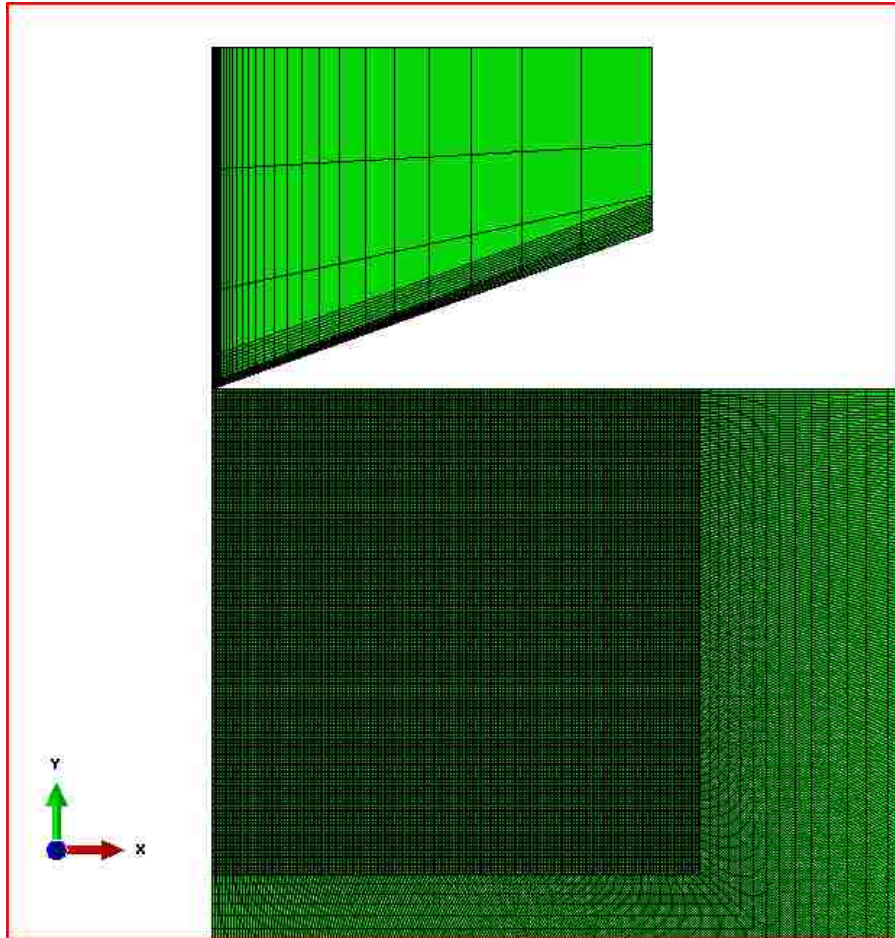


Figure 11: Mesh 2

Mesh 3 (the same mesh shown in Figure 9) was constructed differently from the first two. A bias was used to move the nodes closer to the indentation area in the x -direction. In the y -direction the location of the nodes were manually assigned. In the first section the rows are the closest together; after each section the rows become spaced further apart. For example the first 50 rows are spaced $0.020 \mu m$ apart. The second sections are spaced $0.050 \mu m$ apart. The nodes further from the indentation zone become larger and less uniform than around the indenter. Figure 12 displays a close-up view of the mesh around the indentation site.

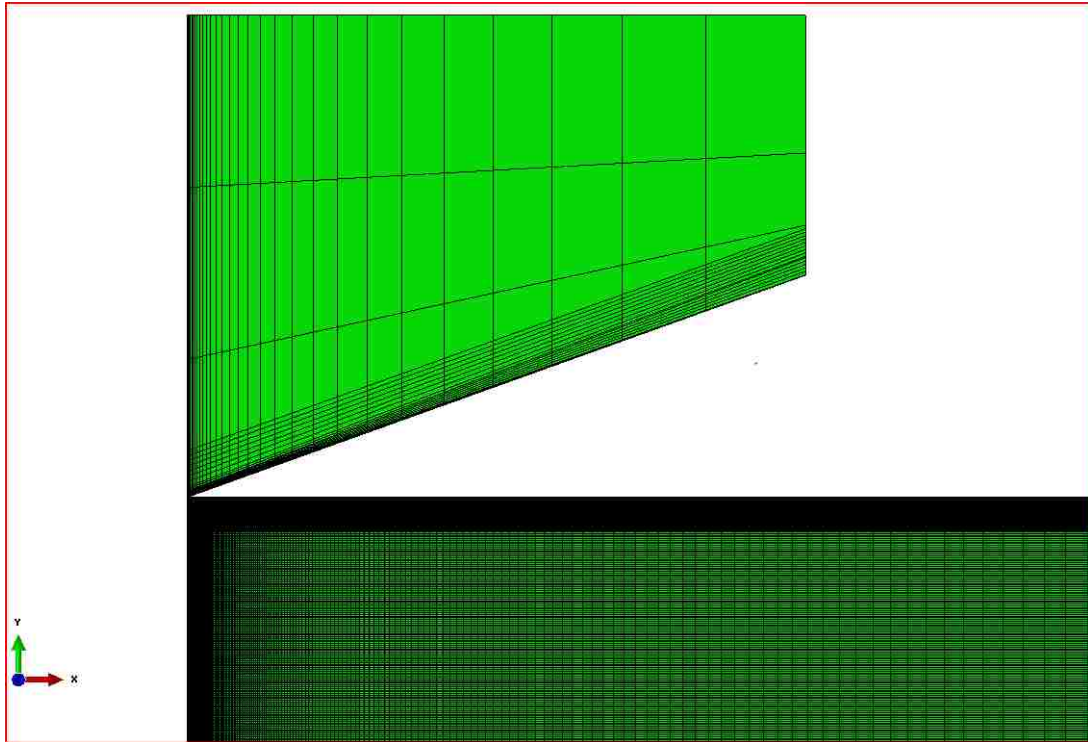


Figure 12: Mesh 3

To test the convergence and justify that any depth can be used with this model to accurately calculate the hardness using indentation, a material was chosen and analyzed at one specific target strain rate. The hardness was calculated at specific depths from $1 - 4\mu m$ for each of the three meshes shown above. It can be seen in Figure 13 that the results from these three meshes are essentially independent of the indentation depth, and the hardness values are all within $10 MPa$ of each other. Therefore the convergence of mesh is confirmed, and Mesh 3 was chosen for all the results in this study.

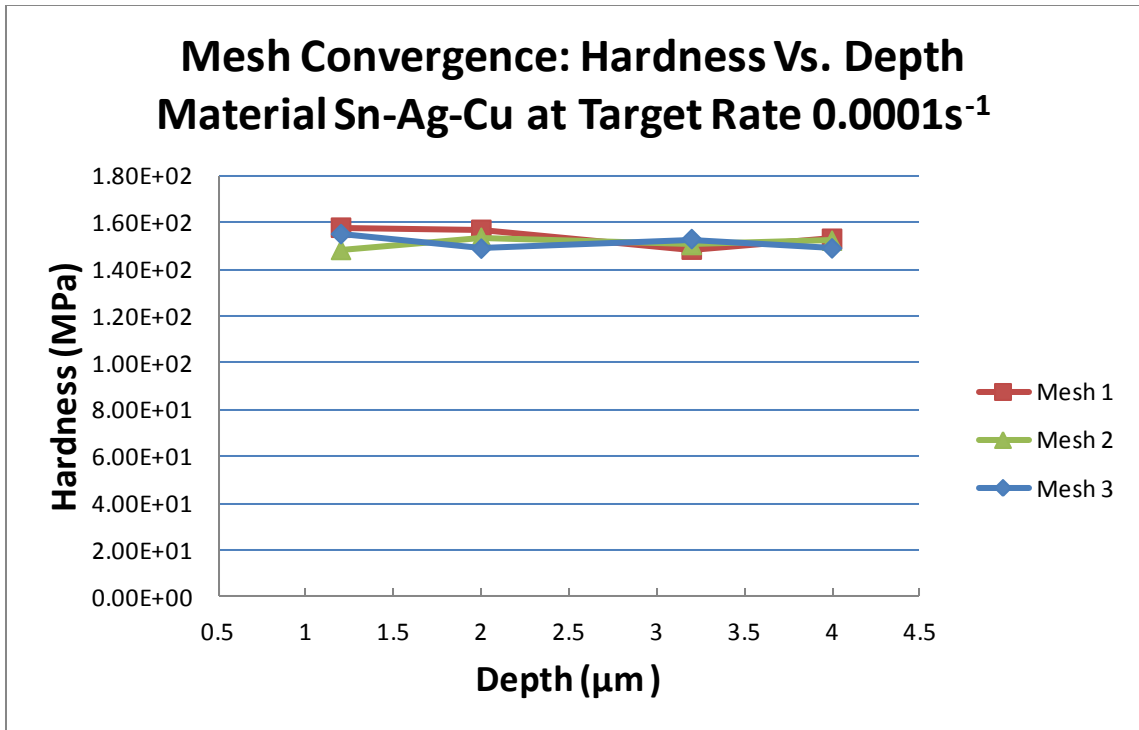


Figure 13: Convergence study

Ch.3 Uniaxial Creep Response

In this chapter we describe and discuss the numerical results of the uniaxial creep response. Again, the objective is to establish a connection between the viscoplastic input and the power-law creep output. A pure tin (Sn) material and Sn based alloys; one at 25°C and another at an elevated 120°C were simulated using the viscoplasticity approach as stated in Section 2.2. Note that the temperature effect is not explicitly built into the model; the strain rate-flow stress relationship at the different temperatures from experiment was directly taken as input in the model. For each material in this uniaxial creep test several loads within the input parameter range were chosen.

At the completion of the finite-element model the overall strain was extracted and plotted against time for each constant applied stress to the specimen, as shown in Figures 14,16,18, and 20. In each case, as expected, there is an “instantaneous” strain or ϵ_0 due to applied stress within 0.01s. The applied stress value will determine the magnitude of ϵ_0 . However, the creep characteristic we are interested in occurs after the instantaneous strain. The steady-state creep strain rate can be extracted from this plot by simply taking the slope of the strain as a function of time after ϵ_0 . When comparing the resulting stress with the strain rate extracted in each simulation, it is shown in Figures 15, 17, 19 and 21 that the output steady-state strain rate directly correlates with the input viscoplasticity response. This direct correlation between the two indeed validates the finite-element model and can then be used to find a relationship between uniaxial creep and indentation creep behaviors.

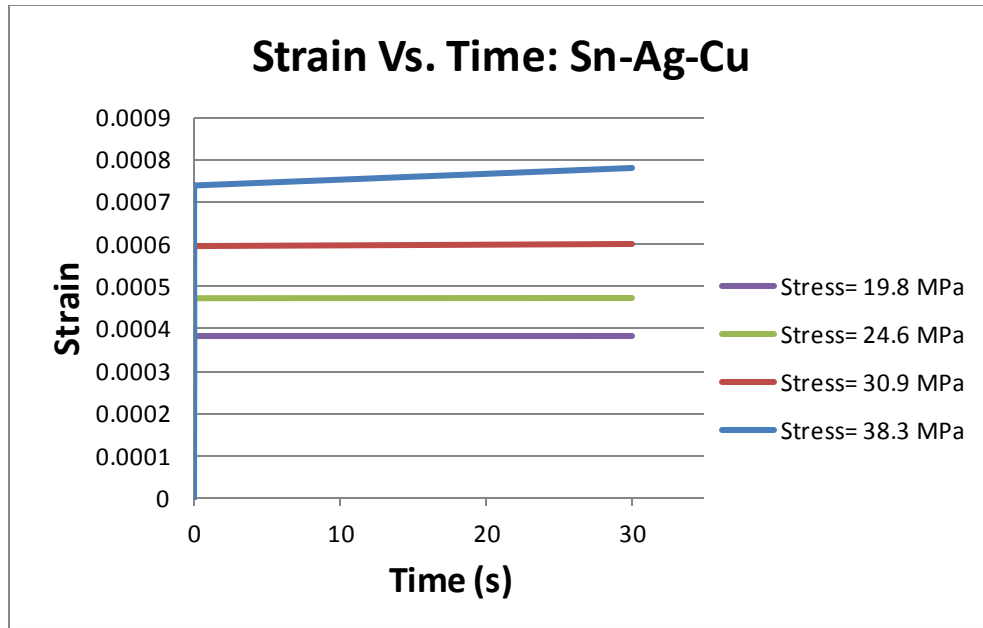


Figure 14: Strain vs. Time with material Sn-Ag-Cu

Figure 14 displays strain as a function of time for four different applied stresses ranging from 19.8 MPa – 38.3 MPa . The slope of each curve (strain rate) is extracted and compared with its corresponding stress as shown in Figure 15. This alloy of Sn-Ag-Cu fits the input data throughout the entire stress range with great accuracy. The output flow stress and steady-state strain rate results closely overlap the input viscoplasticity parameter data in Figure 15.

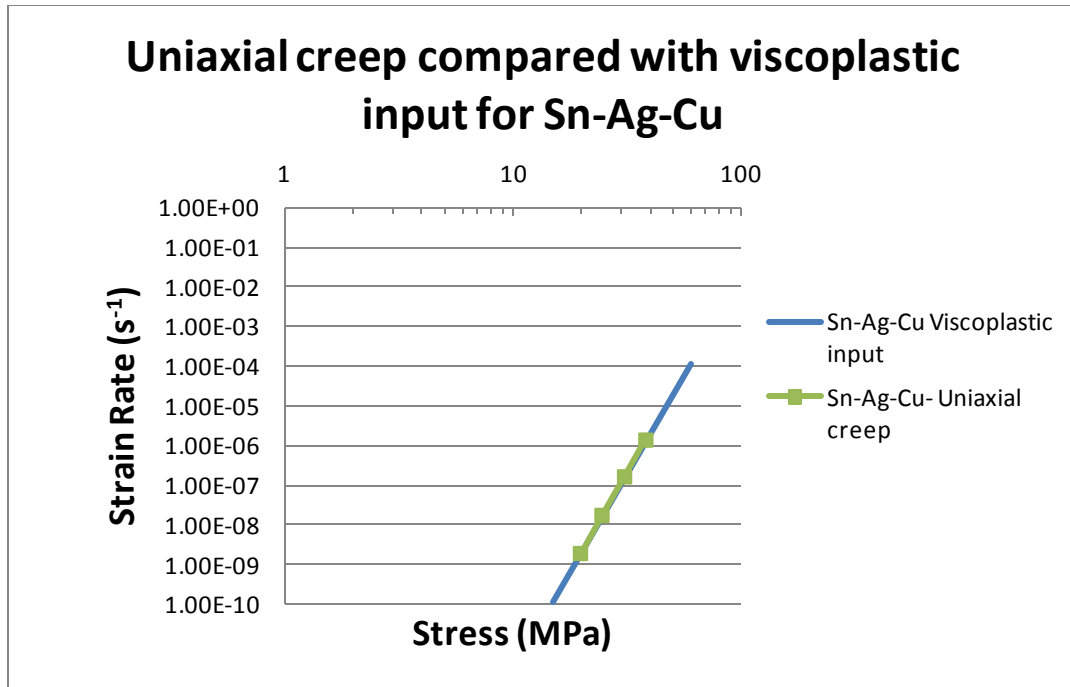


Figure 15: Viscoplastic input compared with uniaxial creep output for Sn-Ag-Cu

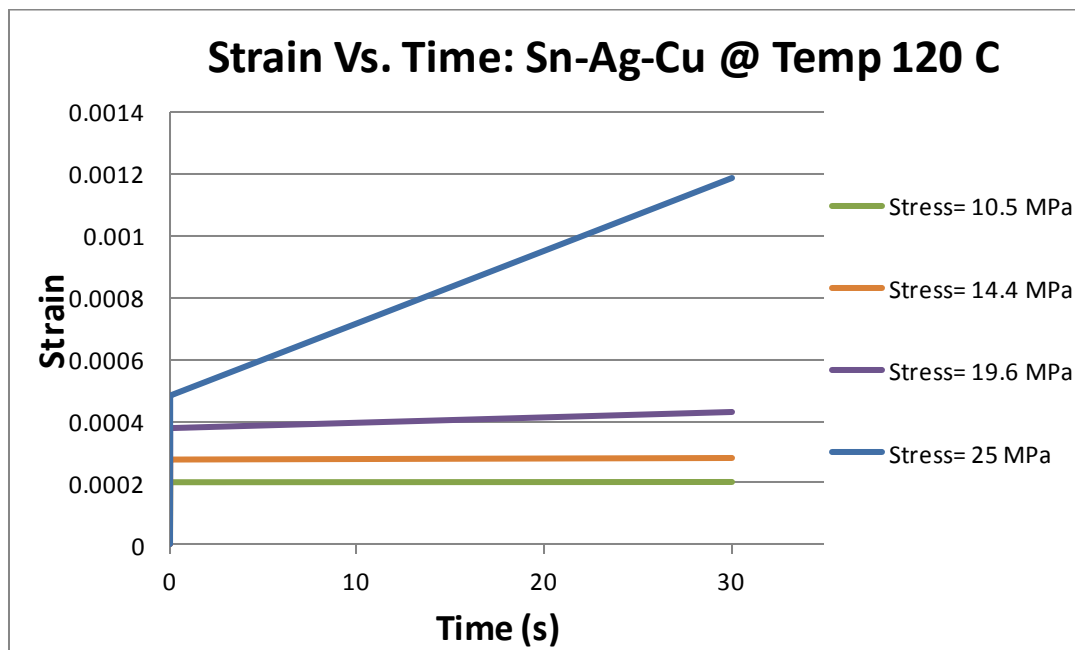


Figure 16: Strain vs. Time with material Sn-Ag-Cu @ 120°C

Figure 16 displays Sn-Ag-Cu at 120°C with an applied stress range from 10.5 MPa – 25 MPa. With this increase in temperature notice that the applied stress range is close to half the applied stress range as the same alloy at 25°C. Figure 17 displays a decrease in flow stress due to the increase in temperature. The extracted strain rate from Figure 16 fits the input data well over the middle stress ranges, as shown in Figure 17. At the extreme bounds, specifically at stresses of 10.5 MPa and 25.0 MPa there is a slight deviation from the input.

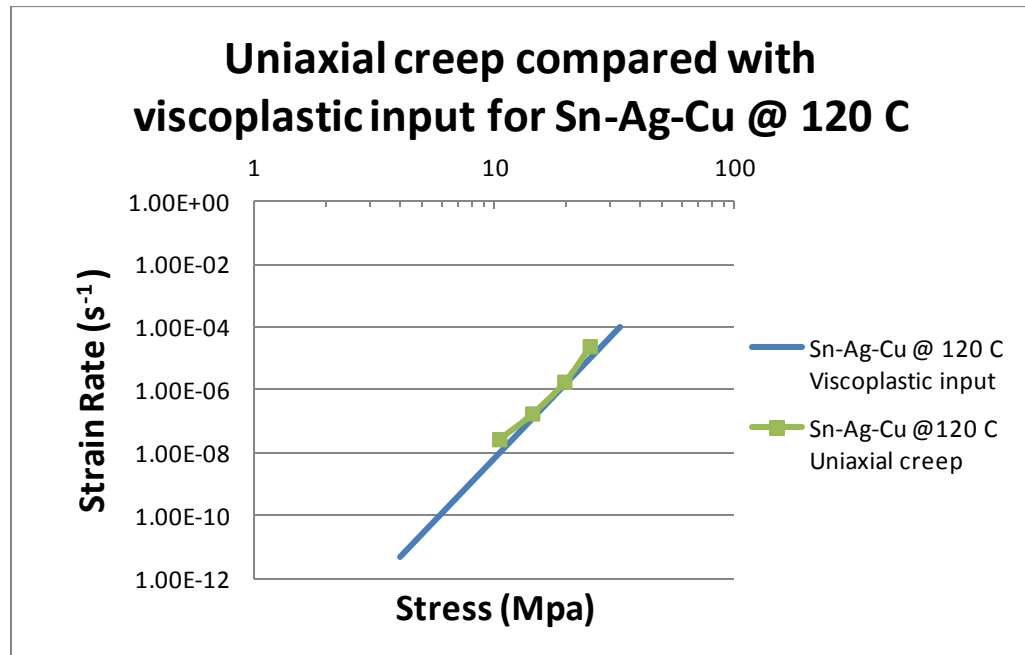


Figure 17: Viscoplastic input compared with uniaxial creep output for Sn-Ag-Cu @ 120°C

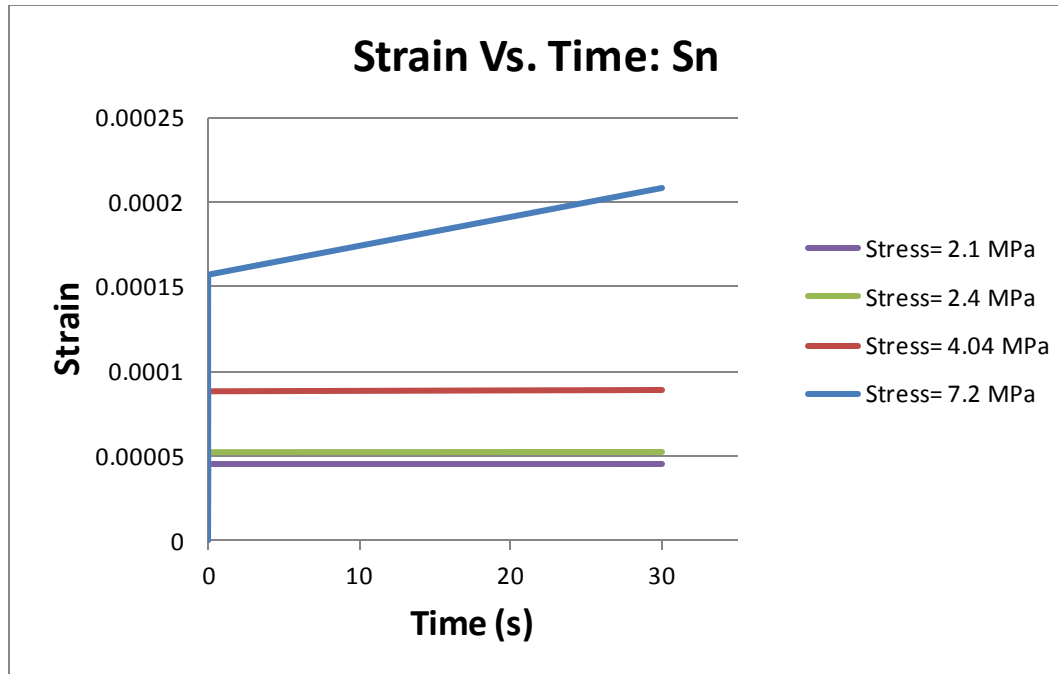


Figure 18: Strain vs. Time with material Sn

Figure 18 displays the pure Sn material at 25°C. When comparing the extracted output strain rate with the input, there is a similar correlation between the two. A fitted curve from the input data throughout all stress ranges can be seen in Figure 19. From the results of materials at room temperature, we observe a very close correlation between input viscoplastic parameters and output strain rate and applied stress.

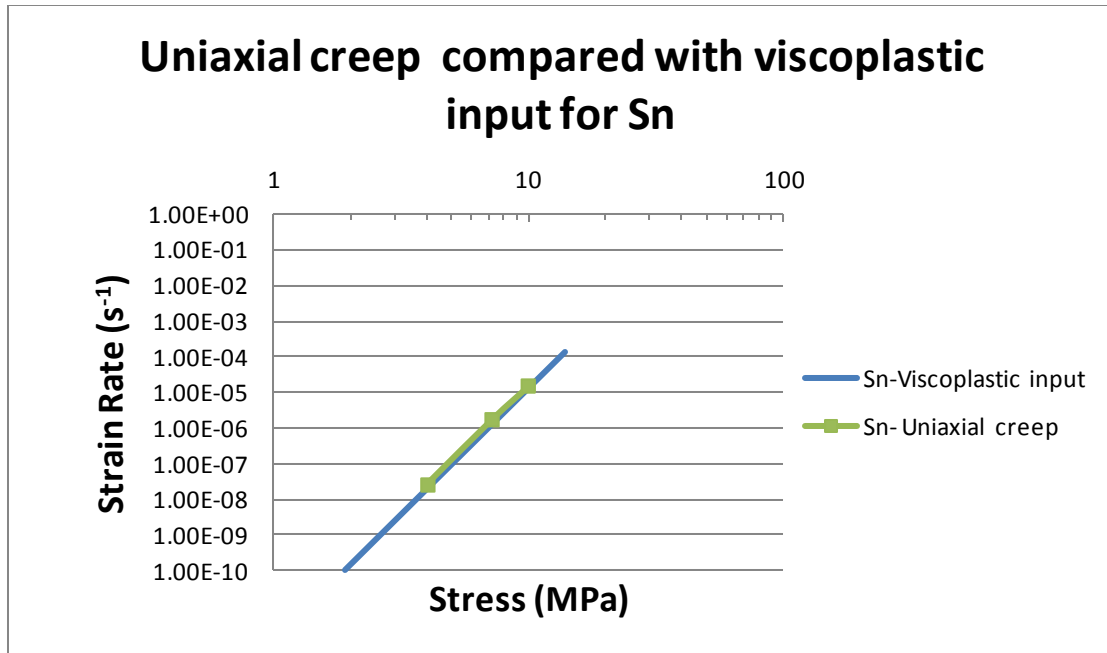


Figure 19: Viscoplastic input compared with uniaxial creep output for Sn

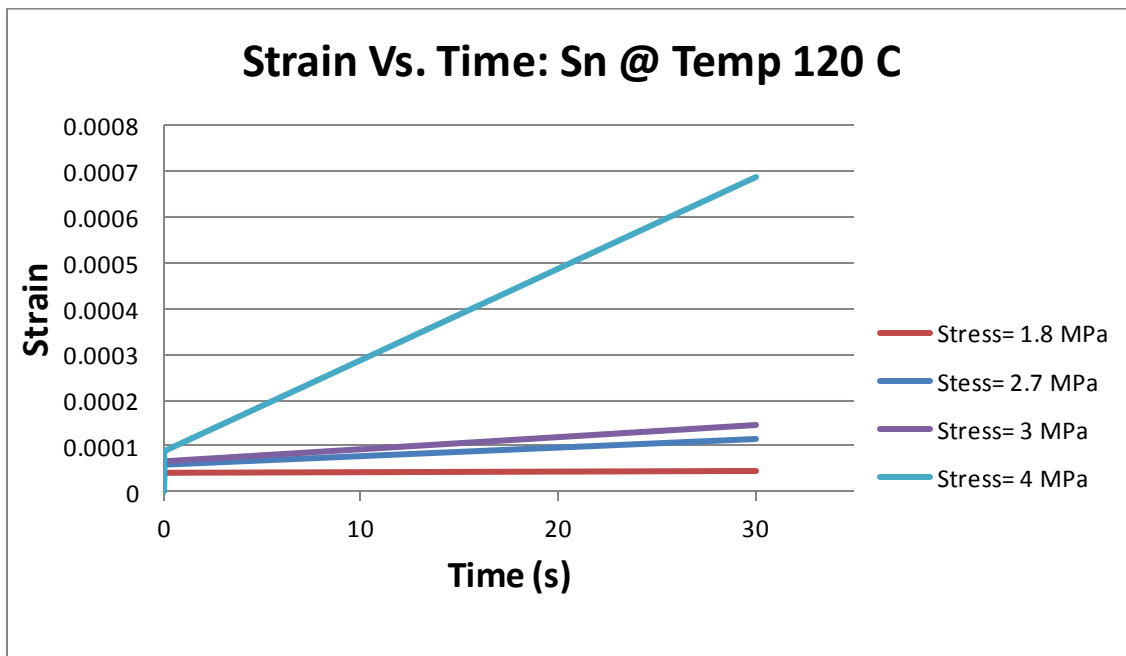


Figure 20: Strain vs. Time with material Sn@120°C

Figure 20 displays the results for pure Sn at 120°C. The stress values for this material and temperature are in the lowest range among all four cases. As seen in Figure 21 the output strain rate and flow stress match well with the input viscoplastic parameters after about 3.0 MPa. Below this stress an offset from the viscoplastic parameter is observed; however, the relation continues along the same slope shown in Figure 21.

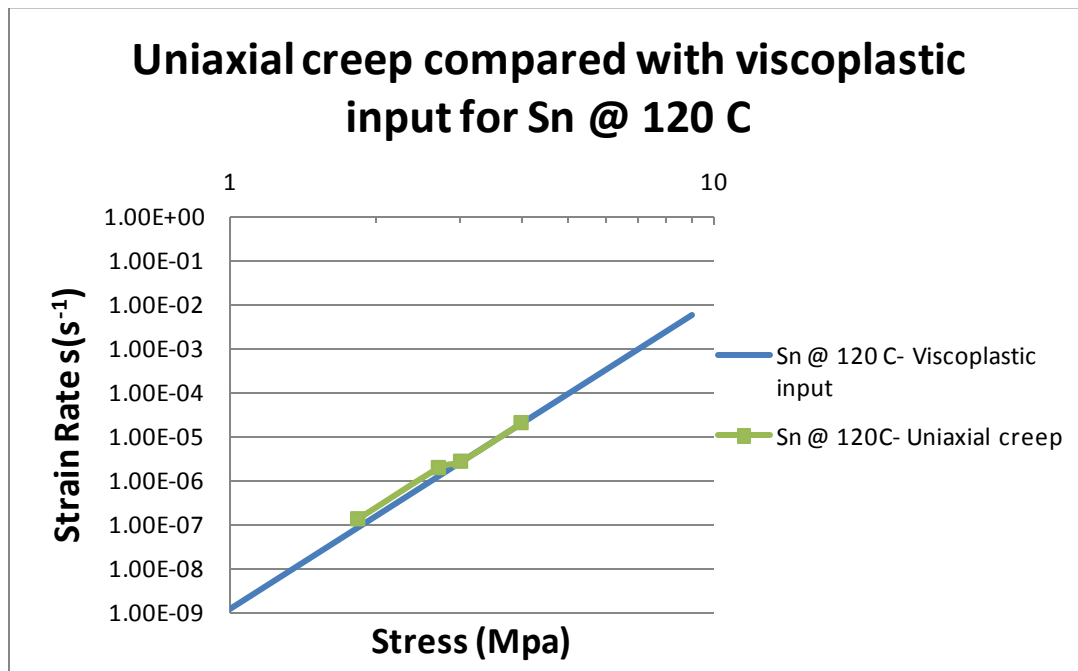


Figure 21: Viscoplastic input compared with uniaxial creep output for Sn@ 120°C

On the basis of the above findings, we conclude that, within the stress and strain rate ranges considered for the Sn and Sn-based alloy, the input viscoplastic model corresponds well with the output uniaxial creep model. This forms the basis for indentation creep analysis in Chapter 4, which employs the same viscoplastic properties as the model input.

Ch.4 Indentation-derived Creep Response

In this chapter we describe and discuss the numerical results of the indentation-derived creep response. The objective is to establish a connection between uniaxial creep and indentation creep. As described in Chapter 1, the comparison of indentation creep data to uniaxial or conventional creep testing is difficult due to the determination of strain rate experienced by the material during indentation [10]. In this study all indentation results are based off a $4\mu\text{m}$ depth indentation. A constant indentation strain rate of loading (Eq.(5)) is applied to the indenter, and the load as a function of depth is extracted for different strain rates as displayed in Figures 22-25. Observe how the load increases with an increase of target strain rate. Using the model to find the maximum load which occurs at $4\mu\text{m}$ depth and dividing by the projected contacted area will calculate the hardness value. The hardness values at the various indentation strain rates are then divided by 3 (Eq.(8)), to obtain the corresponding flow stresses resulting from indentation.

The equivalent plastic strain for the Sn based alloy Sn-Ag-Cu at $25\text{ }^\circ\text{C}$ at a depth of $4\mu\text{m}$ is displayed in Figures 26-29. There is a similarity between all four results unlike the load-depth curves that change with a function of strain rate; the equivalent plastic strain seems to stay relatively constant regardless of the strain rate applied. This suggests the same level of deformation when the tip of the indenter is at the same prescribed depth, irrespective of the widely different strain rates. The “strain rate hardening” effect is better manifested by the contour plots of von Mises effective stress, as shown in Figures 30-33. Here the same material at an independent depth of $4\mu\text{m}$ is

considered. It is evident that, as the applied indentation strain rate increases, the material volume directly underneath the indenter experiences larger stress.

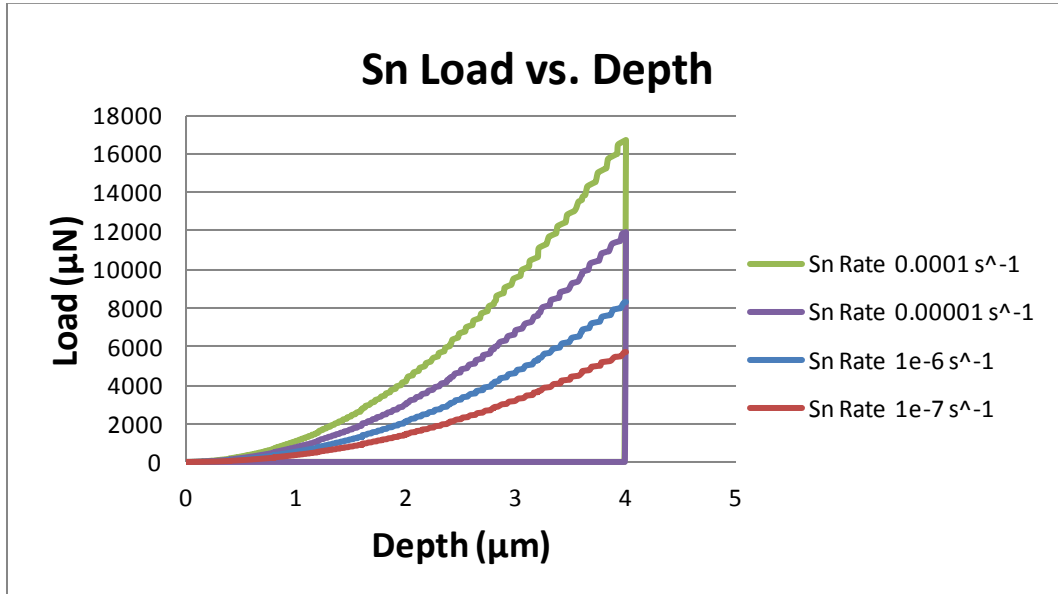


Figure 22: Load vs. Depth for Sn @ varying strain rate

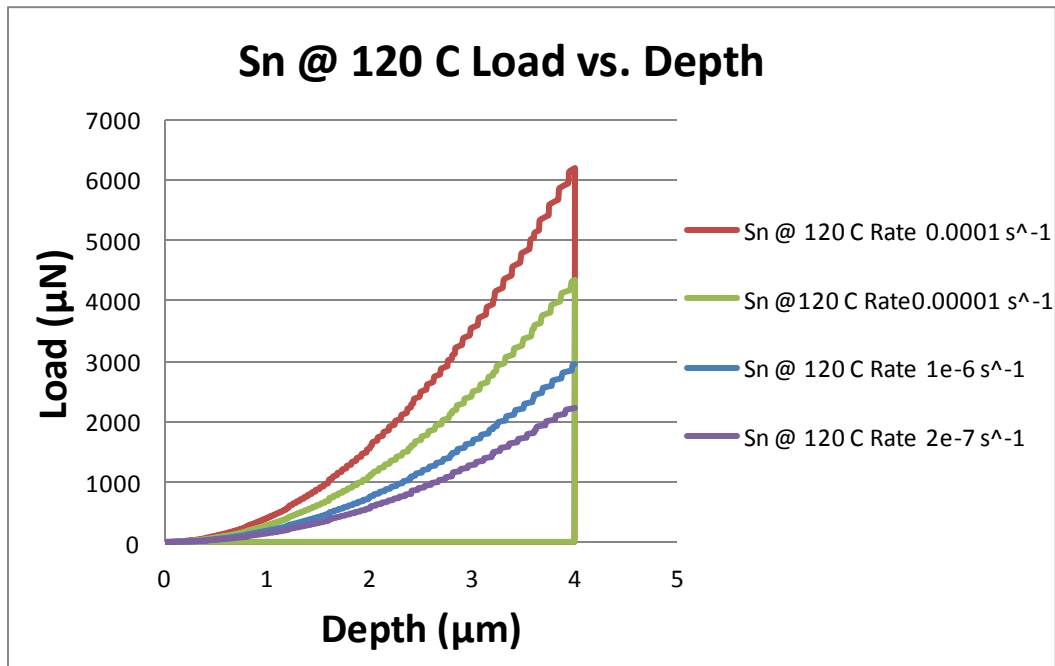


Figure 23: Load vs. Depth for Sn @ 120 °C @ varying strain rate

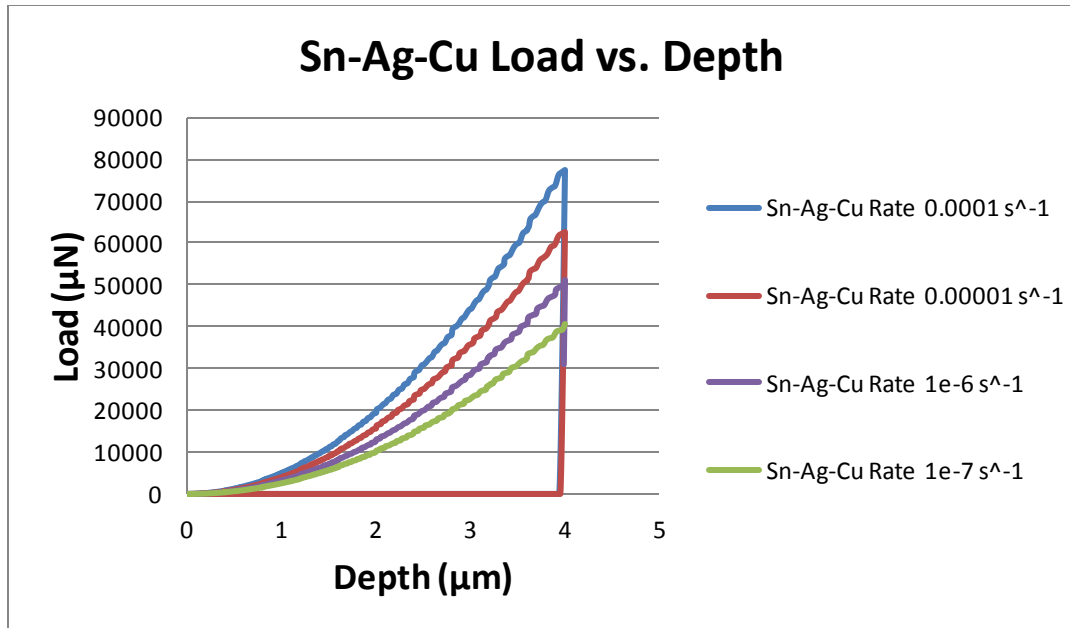


Figure 24: Load vs. Depth for Sn-Ag-Cu @ varying strain rate

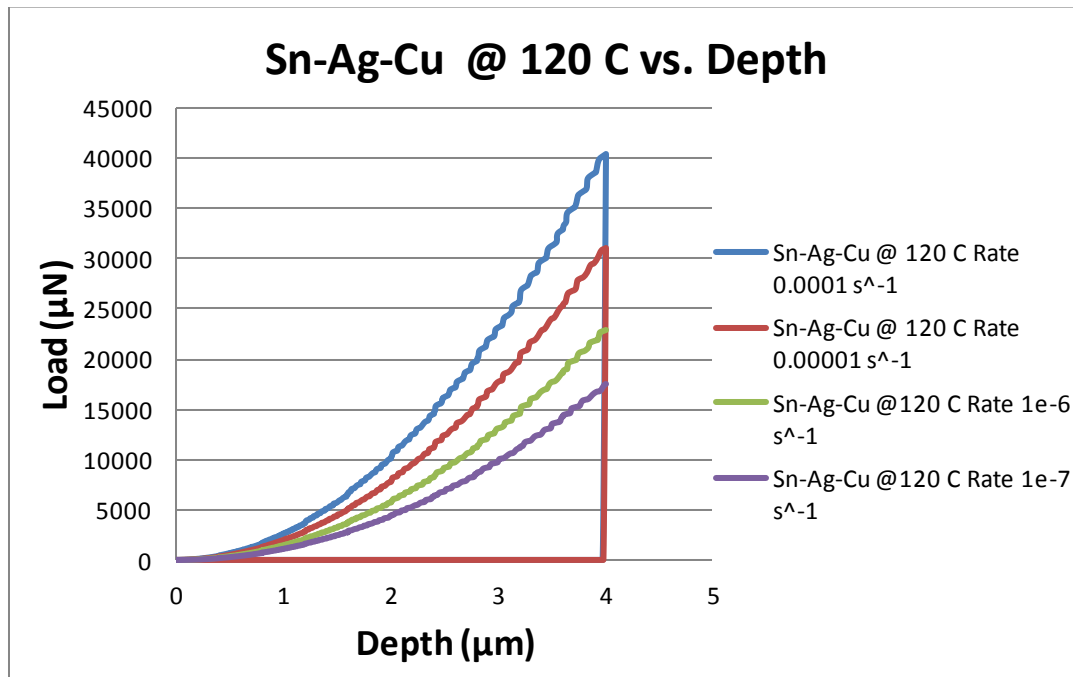


Figure 25: Load vs. Depth for Sn-Ag-Cu @ 120°C @ varying strain rate

Figure 34 displays the simulated indentation strain rate-flow stress relation, and the result is compared with the uniaxial creep response (which serves as the input for the present indentation modeling). Within the range of strain rate considered, the flow stress values of the four materials cover a wide span from about 1.47 MPa to 49.7 MPa. One notable feature is that, the indentation strain rate-stress curves are generally linear, and are nearly parallel to the uniaxial creep response for the respective materials. This makes possible the determination of the quantitative difference between the indentation strain rate and uniaxial strain rate, related by

$$\dot{\varepsilon}_u = C \dot{\varepsilon}_I, \quad (9)$$

where C is a coefficient relating these two strain rates with the subscript I representing indentation and u representing uniaxial.

For the uniaxial steady-state creep behavior of Sn at 120°C, the stress exponent n_c is equal to 6.42, and the indentation creep gives rise to a n_c value of 6.31. The constant C can be calculated from the vertical distance between the two curves. Taking the average distance at the upper and lower ends of the indentation creep curve (since the curves are not exactly parallel), a C value of 0.21 is obtained.

Applying the same approach, the stress exponent n_c and the constant C relating the two strain rates for the other materials can be obtained. The result is summarized in Table 4.

Material	Uniaxial Stress Exponent n_c	Indentation Stress Exponent n_c	C
Sn-Ag-Cu @ 25°C	9.96	10.55	0.28
Sn @ 25°C	7.07	6.53	0.25
Sn-Ag-Cu @ 120°C	7.76	7.67	0.20
Sn @ 120°C	6.42	6.31	0.21

Table 4: Stress exponents for uniaxial and indentation tests

As seen from the Table, a relative consistency between the C coefficients (between 0.20 and 0.28) is observed. Note also that for all Sn alloys and pure Sn tested, the stress exponent n_c resulting from indentation were all within 0.59 difference from the uniaxial value. The present numerical finding of nearly identical stress exponents between indentation creep and uniaxial creep is consistent with previous experimental results [5-6]. The most important contribution of this current study, however, is the quantification of indentation strain rate and uniaxial strain rate for the power-law creep materials considered, which has not been established by other researchers.

Although the present analysis utilizes four Sn-based material systems, it covers a reasonably wide range of flow stress and strain rate so the conclusions should apply to similar types of soft metallic materials. When using indentation creep with constant target indentation strain rates, $\dot{\epsilon}_t$ (Eq.(5) in Chapter 2), a relative consistency of the ratio between uniaxial strain rate and indentation strain rate was achieved (0.20 to 0.28). To a first approximation, a value of 0.24 may be chosen. In practice, one may then use this indentation approach to test a soft alloy with unknown creep property. Plotting the indentation strain rate vs. flow stress as in Figure 34, and then vertically translating the

curve to 24% of its strain rate position, will yield the "uniaxial" creep response of the material. The complete power-law creep property at the testing temperature is then fully determined.

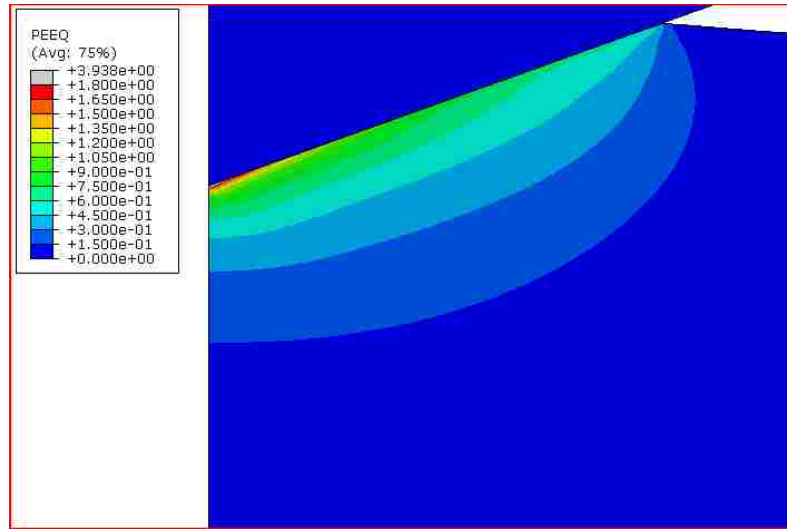


Figure 26: Equivalent plastic strain for Sn-Ag-Cu @ Rate $0.0001s^{-1}$

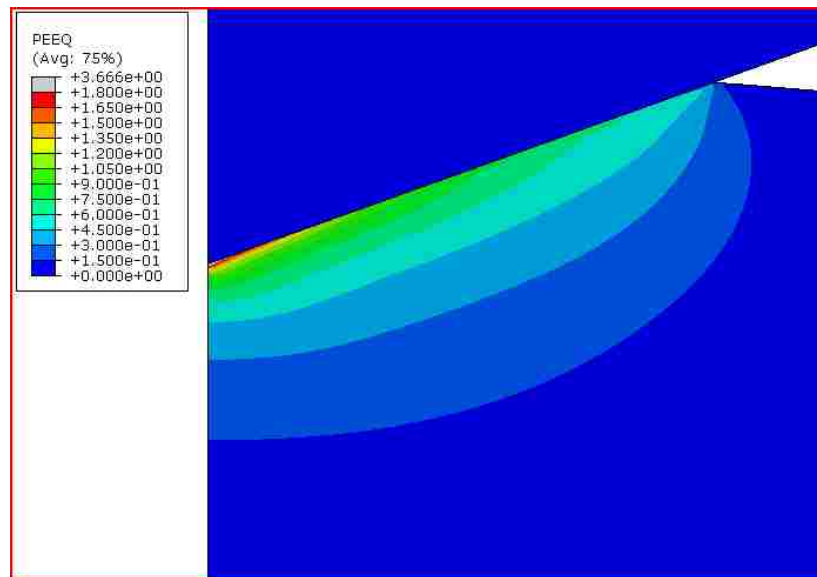


Figure 27: Equivalent plastic strain for Sn-Ag-Cu @ Rate $0.00001s^{-1}$

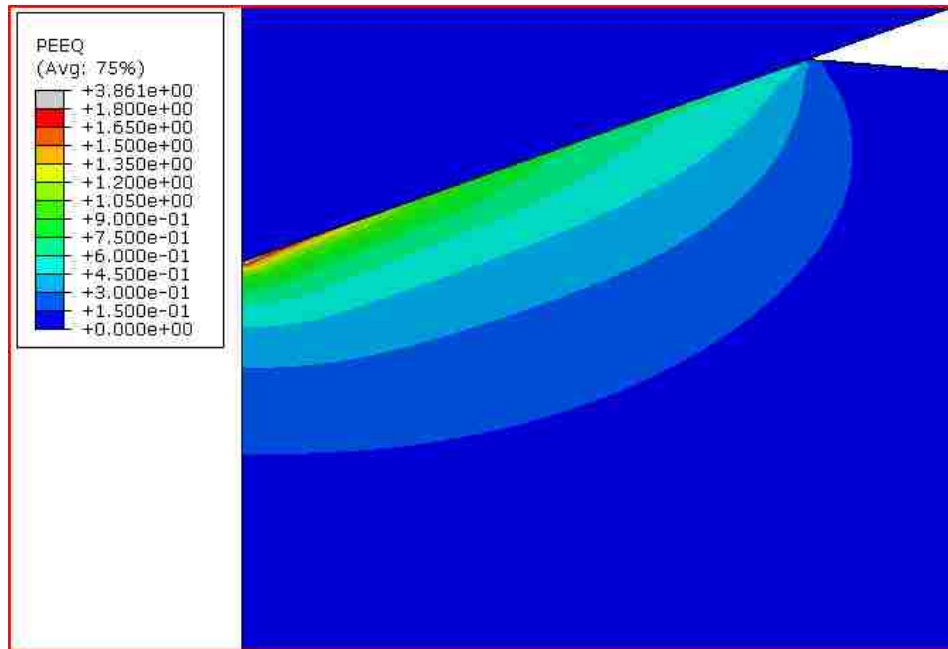


Figure 28: Equivalent plastic strain for Sn-Ag-Cu @ Rate $1 \times 10^{-6} s^{-1}$

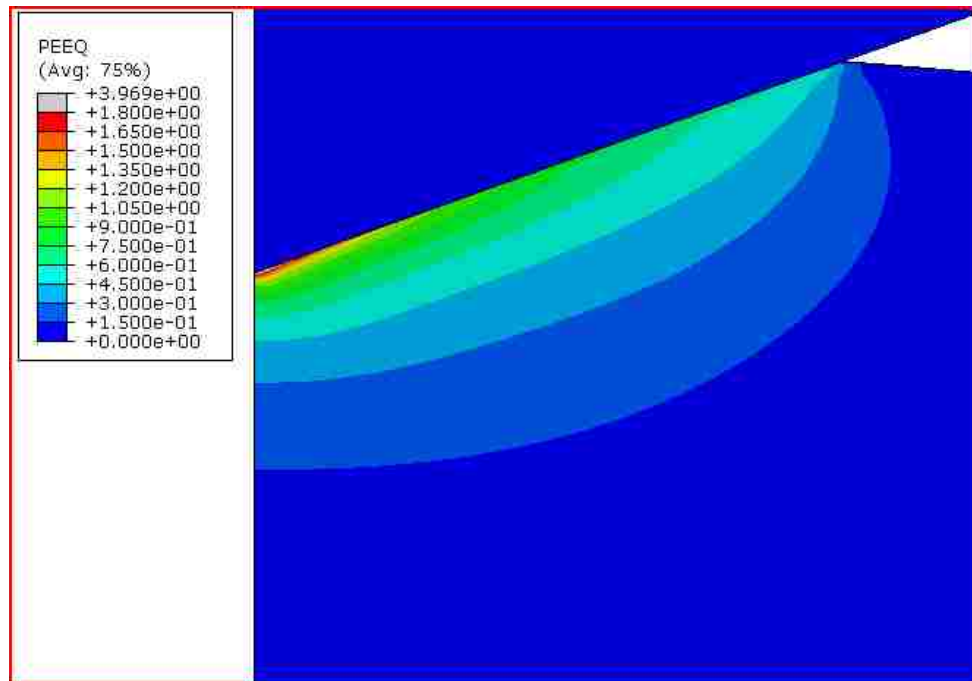


Figure 29: Equivalent plastic strain for Sn-Ag-Cu @ Rate $1 \times 10^{-7} s^{-1}$

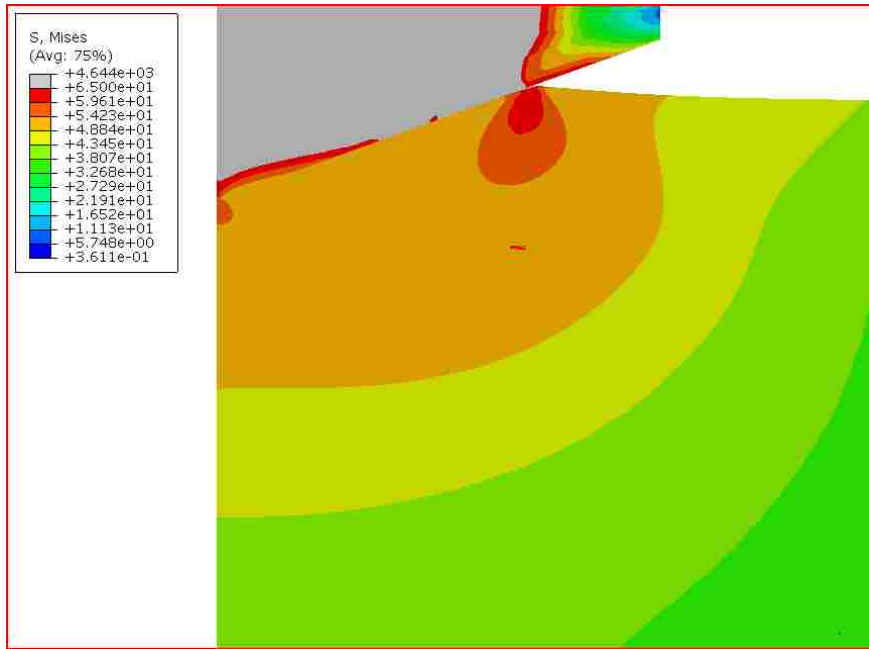


Figure 30: Von Mises Stress (in MPa) For Sn-Ag-Cu @ Rate $0.0001s^{-1}$

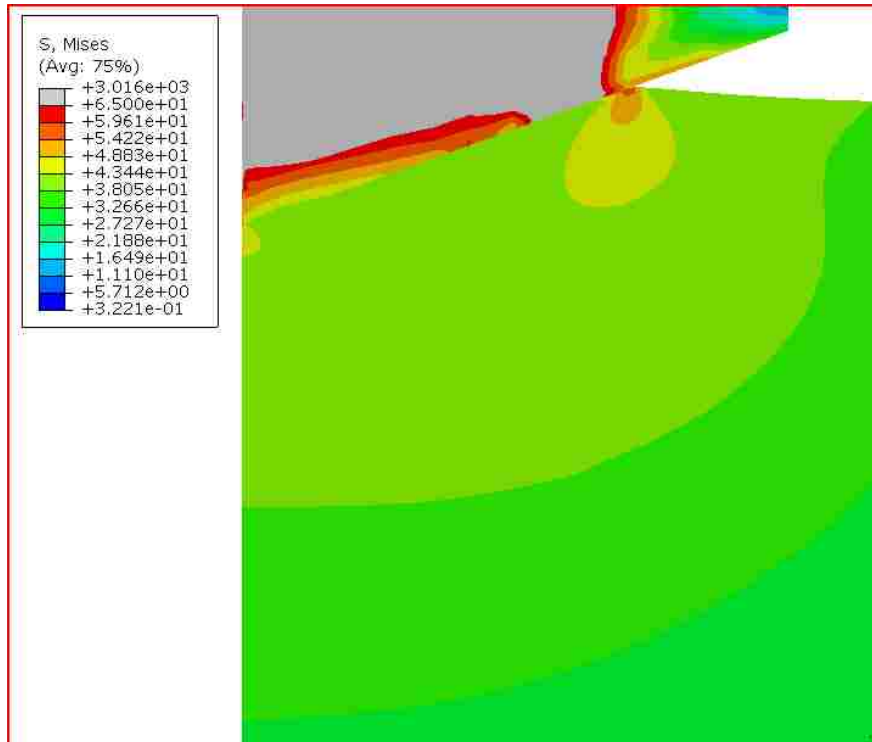


Figure 31: Von Mises Stress (in MPa) For Sn-Ag-Cu @ Rate $0.00001s^{-1}$

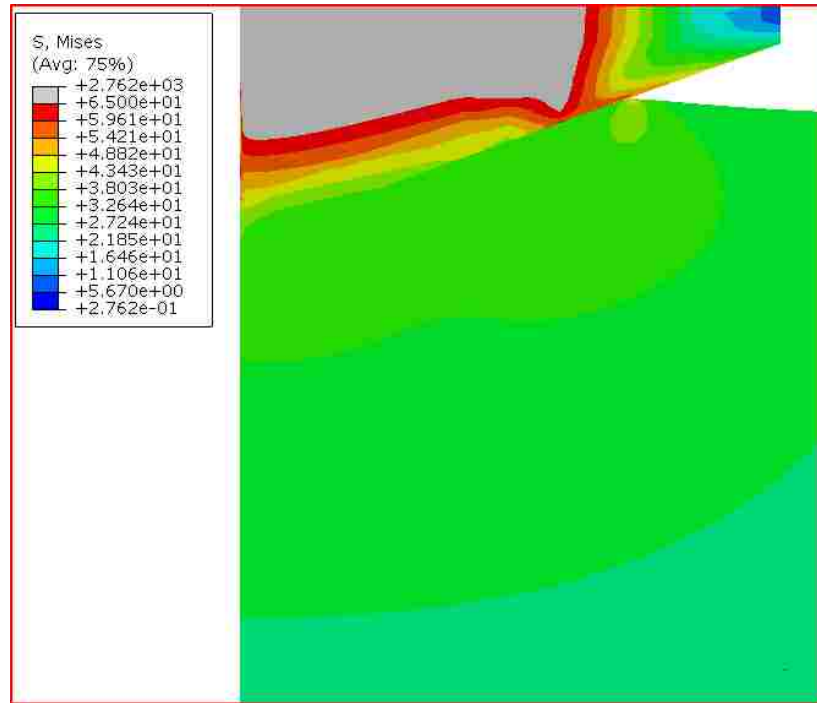


Figure 32: Von Mises Stress (in MPa) For Sn-Ag-Cu @ Rate $1.0 \times 10^{-6} s^{-1}$

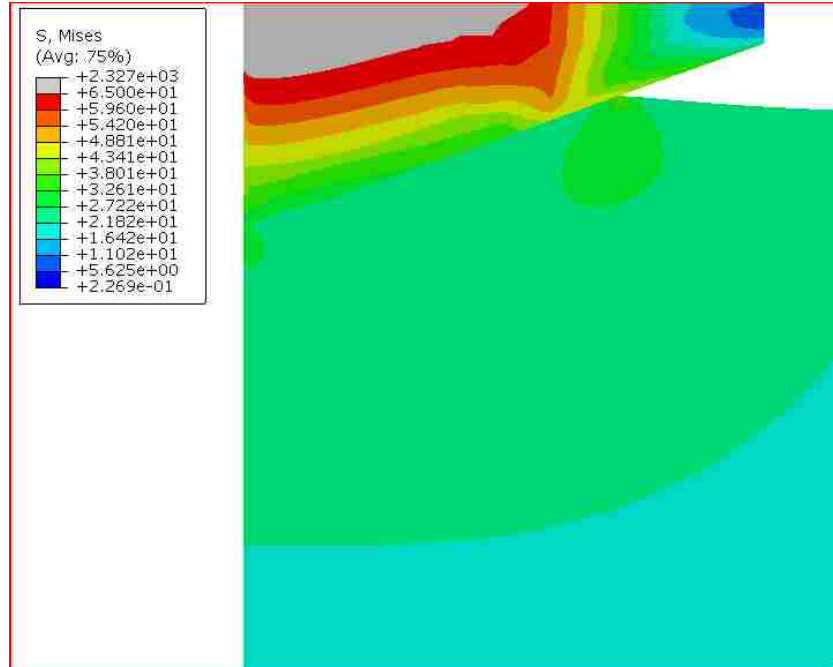


Figure 33: Von Mises Stress (in MPa) For Sn-Ag-Cu @ Rate $1.0 \times 10^{-7} s^{-1}$

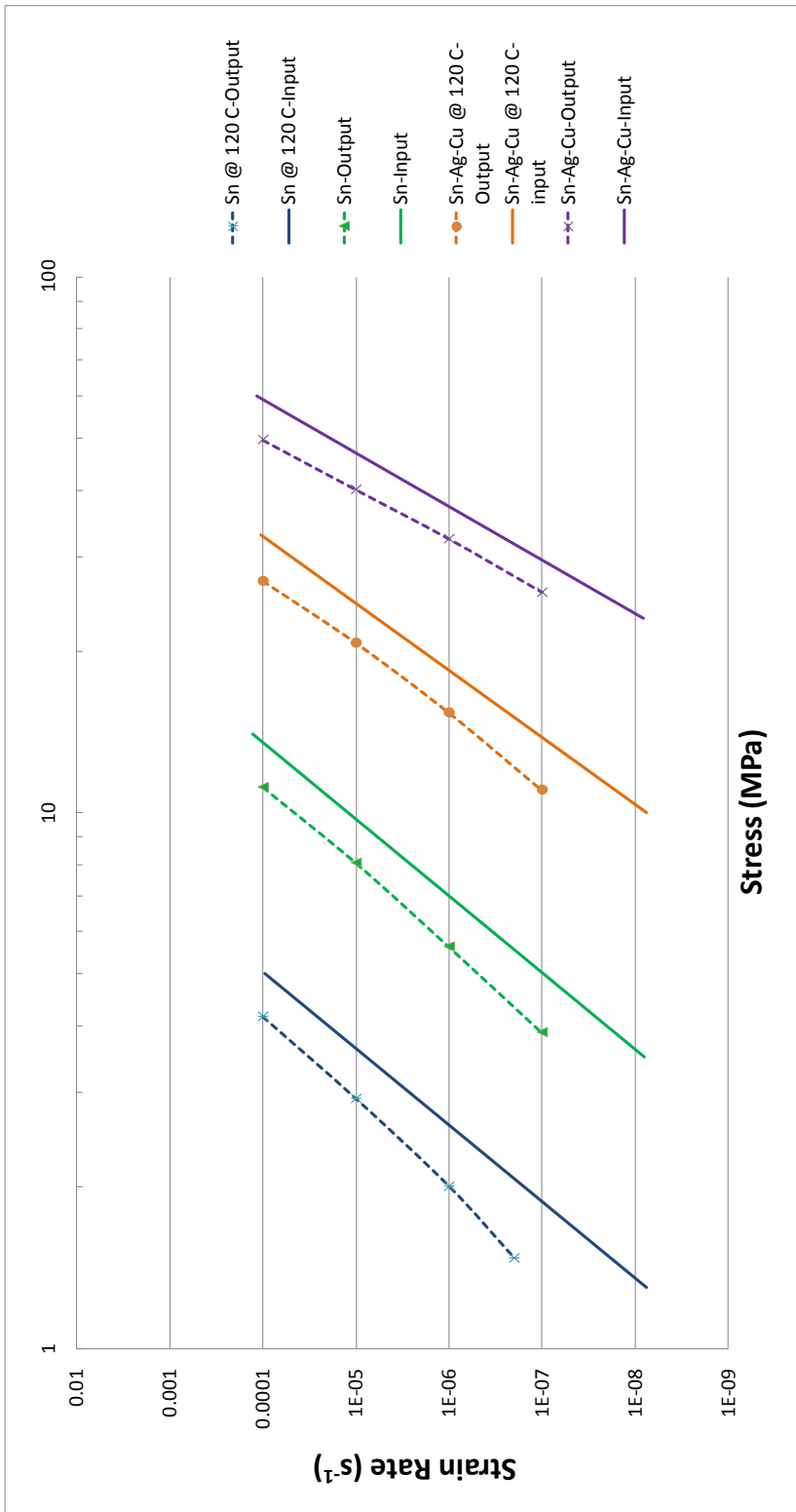


Figure 34: Steady state strain rate compared with uniaxial strain rate and stress

Ch.5 Conclusions and Suggested Future Work

5.1 Conclusions

In this study the time-dependent properties of pure Sn and Sn-based solder alloys were investigated using numerical finite element modeling. Attention is directed to identifying the relationship between indentation creep and uniaxial power-law creep, specifically the quantitative relationship between indentation strain rate and uniaxial strain rate obtained from conventional creep test. There has yet to be a validated method for such correlation.

This study involves two stages of numerical simulation, the first a uniaxial creep test and the other an indentation test. Both were based on rate-dependent viscoplastic behavior as the input material model for the pure Sn and Sn alloys. A series of constant-load creep test was first simulated. The viscoplastic approach was found to yield the same steady-state strain rates under the corresponding applied stresses on the uniaxial creep model, thus validating the use of viscoplasticity for creep modeling. The same viscoplastic approach was then employed in indentation creep analyses.

The indentation loading is based on a constant indentation strain rate, defined as \dot{h}/h , with h being the instantaneous depth, for geometrically similar indenter shapes. The hardness as a function of indentation strain rate was obtained for the model materials considered and converted to flow stress. The stress exponent n_c of the power-law creep expression can thus be determined, and it was found to be nearly identical to the stress exponent in conventional uniaxial creep. This similar stress exponent gives rise to a near parallel strain rate-flow stress curves (on the logarithmic scale) between uniaxial creep and indentation creep. The separation between the curves thus provides the strain rate

relationship between uniaxial creep and indentation creep. A relative consistent ratios between uniaxial and indentation strain rates, from 0.20 to 0.28, was obtained. An approximate value of 0.24 may be chosen, to translate the indentation strain rate-flow stress curve to “match” the corresponding uniaxial response. In practice this indentation technique can be applied to soft alloys with unknown power-law creep properties. Their uniaxial creep parameters, valid over the same range of strain rate and flow stress considered in the present study, can thus be fully characterized.

5.2 Suggested future studied

The current study focuses on four model materials with the stress exponent ranging between 6.31 and 10.55. Extending the analyses to cover materials with other exponents will be a worthwhile effort. (Note that one can numerically study the case of amorphous Se [14] and compare the result with experiment.)

While this research utilized published uniaxial creep data as a basis [9], a self-sufficient experimental study may be conducted. Commercial pure Sn and/or Sn-based alloys may be acquired for the constant-stress uniaxial creep test and the instrumented indentation test. Systematic sets of strain rate and flow stress data can then be plotted in the same way as in the present numerical analysis, to reveal the quantitative relationship between the indentation strain rate and uniaxial strain rate during creep.

Further explorations may include alloy systems with higher strengths under a wide temperature (and thus strain rate) ranges. This may be carried out experimentally and/or numerically. Complications may arise due to the possibly different dominant creep mechanisms (climb-assisted dislocation glide, grain boundary diffusion, lattice diffusion,

and grain boundary sliding etc.) even in a given indentation test. Nevertheless, there will always be a quantitative relation between the indentation strain rate and uniaxial strain rate. The generality of such a relation can therefore be thoroughly tested.

References

- [1] Liu, C., & Chen, J. (2007). Nanoindentation of lead-free solders in microelectronic packaging. *Materials Science and Engineering A*, 448(1-2), 340-344.
- [2] Yang, H., Deane, P., Magill, P., & Murty, K, L. (1996). Creep deformation of 96.5 Sn-3.5 Ag Solder Joints in a Flip Chip Package. *Electronic Components and Technology Conference*, 46, 1136-1142.
- [3] Shen, L., Septiwerdani, P., & Chen, Z. (2012). Elastic modulus, hardness and creep performance of SnBi alloys using nanoindentation. *Materials Science & Engineering A*, 558, 253-258.
- [4] Yang, H., Deane, P., Magill, P., & Murty, K. L. (1996). Creep deformation of 96.5 Sn-3.5 Ag solder joints in a flip chip package. *Electronic Components and Technology Conference*, 46, 1136-1142.
- [5] Mahmudi, R., Geranmayeh, A. R., & Rezaee-Bazzaz, A. (2007). Impression creep behavior of lead-free Sn-5Sb solder alloy. *Materials Science and Engineering A*, 448(1-2), 287-293.
- [6] Huang, M. L., Wang, L., & Wu, C. (2002). Creep behavior of eutectic Sn-Ag lead-free solder alloy. *Journal Of Materials Research*, 17(11), 2897-2903.
- [7] Sidhu, R. S., Deng, X., & Chawla, N. (2008). Microstructure characterization and creep behavior of Pb-free Sn-rich solder alloys: Part II. Creep behavior of bulk solder and solder/copper joints. *Metallurgical and Materials Transactions A*, 39A(2), 349-362.
- [8] Dutta, I., Park, C., & Choi, S. (2004). Impression creep characterization of rapidly cooled Sn-3.5Ag solders. *Materials Science And Engineering A*, 379, 401-410.
- [9] Chawla, N. (2009). Thermomechanical behavior of environmentally benign Pb-free solders. *International Materials Reviews*, 54(6), 368-384.
- [10] Wang, C. L., Lai, Y. H., Huang J.C., & Nieh, T., G. (2010) Creep of nanocrystalline nickel: A direct comparison between uniaxial and nanoindentation creep. *Scripta Materialia*, 62, 175-178.
- [11] Shen, L., Cheong, W, C, D., Foo, Y, L., & Zhong, C. (2012). Nanoindentation creep of tin and aluminium: A comparative study between constant load and constant strain rate methods. *Materials Science & Engineering A*, 532, 505-510.
- [12] Yazzie, K. E., Williams, J. J., & Chawla, N. (2012). Fracture behavior of Sn-3.5Ag-0.7Cu and pure Sn Solders as a function of applied strain rate. *Journal of Electronic Materials*, 42(9), 2519-2526.
- [13] Lucas, B. N., & Oliver, W. C. (1999). Indentation power-law creep of high-purity indium. *Metallurgical And Materials Transactions A*, 30(A), 601-610.

- [14] Poisl, W. H., Oliver, W. C., & Fabes, B. D. (1995). The relationship between indentation and uniaxial creep in amorphous selenium. *Journal Of Materials Research*, *10*(8), 2024-2032.
- [15] Li, W. B., Henshall, J. L., Hooper, R. M., & Easterling, K. E. (1991). The mechanisms of indentation creep. *Acta Metallurgica et materialia*, *39*(12), 3099-3110.
- [16] Meyers M., & Chawla, K. (2009). *Mechanical behavior of materials*. New York, NY: Cambridge University Press.
- [17] Shen, L., Lu, P., Wang, S., & Chen, Z. (2013). Creep behaviour of eutectic SnBi alloy and its constituent phases using nanoindentation technique. *Journal of Alloys and Compounds*, *574*, 98-103.
- [18] Su, C., Herbert, E., Sohn, S., LaManna, J. A., Oliver, W., & Pharr, G. (2013). Measurement of power-law creep parameters by instrumented indentation methods. *Journal of The Mechanics and Physics of Solids*, *61*(2), 517-536.
- [19] Shen Y-L. (2010) *Constrained Deformation of Materials*. New York, NY: Springer Science.
- [20] ABAQUS, Version 6.12.1, Abaqus, Inc., Pawtucket, RI.
- [21] "Coefficient for Static Friction of steel." Carbidedepot.com. (2014). September 1, 2013 <http://www.carbidedepot.com/formulas-frictioncoefficient.htm>
- [22] Mayo, M. J., Siegel, R. W., Narayanasamy, A., & Nix, W. D. (1990). Mechanical properties of nanophase TiO₂ as determined by nanoindentation. *Journal Of Materials Research*, *5*(5), 1073-1082.
- [23] Tabor D. (1951). *The Hardness of Metals*. Oxford, Clarendon Press.

Appendix

A: Uniaxial Creep

Input File for Sn @ Rate $0.0001s^{-1}$

```
20, 1.0, 0.75
*HEADING 21, 0.0, 1.0
Test problem, to make sure input=output 22, 0.25, 1.0
** Define x and y coords. of nodal 23, 0.5, 1.0
points 24, 0.75, 1.0
*NODE 25, 1.0, 1.0
1, 0.0, 0.0
2, 0.25, 0.0
3, 0.5, 0.0
4, 0.75, 0.0
5, 1.0, 0.0
6, 0.0, 0.25
7, 0.25, 0.25
8, 0.5, 0.25
9, 0.75, 0.25
10, 1.0, 0.25
11, 0.0, 0.5
12, 0.25, 0.5
13, 0.5, 0.5
14, 0.75, 0.5
15, 1.0, 0.5
16, 0.0, 0.75
17, 0.25, 0.75
18, 0.5, 0.75
19, 0.75, 0.75
** Define node sets
*NSET, NSET=LEFT, GENERATE
1, 21, 5
*NSET, NSET=BOTTOM,
GENERATE
1, 5, 1
*NSET, NSET=TOP, GENERATE
21, 25, 1
*NSET, NSET=TOPNTIP, GENERATE
21, 24, 1
*NSET, NSET=RIGHT, GENERATE
5, 25, 5
*NSET, NSET=RIGHTNTIP,
GENERATE
5, 20, 5
*NSET, NSET=TIP
25
*NSET, NSET=ALL, GENERATE
1, 25, 1
```

```

**
**
** Define the first element
**ELEMENT, TYPE=cax4
1, 1, 2, 7, 6
** Generate all the other elements
**ELGEN, ELSET=whole
1, 4, 1, 1, 4, 5, 4
** Define element sets
**ELSET, ELSET=lower, generate
1,12,1
**ELSET, ELSET=upper, generate
13,16,1
**
** "Tie" the 2-direction displacements
of the top nodes
** to that of the "tip" node, for
convenience.
**EQUATION
2
TOPNTIP, 2, 1.0, 25, 2, -1.0
**EQUATION
**2
**RIGHNTIP, 1, 1.0, 25, 1, -1.0
**
**SOLID SECTION, ELSET=upper,
MATERIAL=sn
**SOLID SECTION, ELSET=lower,
MATERIAL=sn
**
**
**MATERIAL, NAME=sn
**ELASTIC
46000.0, 0.34
**Plastic
1.9,0.0
**10.0,0.3
**rate dependent,type=yield ratio
1.0, 0.0
1.0, 1.107e-10
1.05,1.585e-10
1.11,2.230e-10
2.11,2.028e-8
3.16, 3.46e-7
4.21, 2.597e-6
4.73, 5.922e-6
5.79, 2.413e-5
7.37,1.31e-4
**
**
**BOUNDARY
LEFT, 1
BOTTOM, 2
**
**
**STEP, AMPLITUDE=RAMP,
INC=10000, NLGEOM

```

```

*STATIC
0.001,0.01,1e-30,0.01
**
** Concentrated load
*cload
TIP, 2, 31.4
**
*OUTPUT,FIELD,variables=preselect,
frequency=1000
*OUTPUT,HISTORY,variables=preselect,
frequency=1
*NODE OUTPUT, NSET=tip
u2,cf
*EL PRINT, ELSET=whole,
POSITION=CENTROID,
FREQUENCY=1000
s11, s22, s33, press, mises, peeq
*NODE PRINT, NSET=tip,
FREQUENCY=1
U1, u2,cf
*END STEP
**

*STEP, INC=10000, NLGEOM
*STATIC
0.000001,30,1e-30,30
**
** Concentrated load
*cload
TIP, 2, 31.4
**
*OUTPUT,FIELD,variables=preselect,
frequency=10
*OUTPUT,HISTORY,variables=preselect,
frequency=1
*NODE OUTPUT, NSET=tip
u2,cf
*EL PRINT, ELSET=whole,
POSITION=CENTROID,
FREQUENCY=1000
s11, s22, s33, press, mises, peeq
*NODE PRINT, NSET=tip,
FREQUENCY=1
U1, u2,cf
*END STEP
**

```

B: Indentation Creep

Input File for Sn @ Rate $0.0001s^{-1}$

```
*Heading 4501, 0.0,-0.360
*Preprint, echo=no, model=no, 4751, 0.0,-0.380
history=no 5001, 0.0,-0.400
** 5251, 0.0,-0.420
***NODE INFORMATION 5501, 0.0,-0.440
** Material nodes 5751, 0.0,-0.460
*node, nset=left 6001, 0.0,-0.480
1, 0.0,0.000 6251, 0.0,-0.500
251, 0.0,-0.020 6501, 0.0,-0.520
501, 0.0,-0.040 6751, 0.0,-0.540
751, 0.0,-0.060 7001, 0.0,-0.560
1001, 0.0,-0.080 7251, 0.0,-0.580
1251, 0.0,-0.100 7501, 0.0,-0.600
1501, 0.0,-0.120 7751, 0.0,-0.620
1751, 0.0,-0.140 8001, 0.0,-0.640
2001, 0.0,-0.160 8251, 0.0,-0.660
2251, 0.0,-0.180 8501, 0.0,-0.680
2501, 0.0,-0.200 8751, 0.0,-0.700
2751, 0.0,-0.220 9001, 0.0,-0.720
3001, 0.0,-0.240 9251, 0.0,-0.740
3251, 0.0,-0.260 9501, 0.0,-0.760
3501, 0.0,-0.280 9751, 0.0,-0.780
3751, 0.0,-0.300 10001, 0.0,-0.800
4001, 0.0,-0.320 10251, 0.0,-0.820
4251, 0.0,-0.340
```

10501, 0.0,-0.840	17251, 0.0,-1.950
10751, 0.0,-0.860	17501, 0.0,-2.000
11001, 0.0,-0.880	17751, 0.0,-2.050
11251, 0.0,-0.900	18001, 0.0,-2.100
11501, 0.0,-0.920	18251, 0.0,-2.150
11751, 0.0,-0.940	18501, 0.0,-2.200
12001, 0.0,-0.960	18751, 0.0,-2.250
12251, 0.0,-0.980	19001, 0.0,-2.300
12501, 0.0,-1.000	19251, 0.0,-2.350
12751, 0.0,-1.050	19501, 0.0,-2.400
13001, 0.0,-1.100	19751, 0.0,-2.450
13251, 0.0,-1.150	20001, 0.0,-2.500
13501, 0.0,-1.200	20251, 0.0,-2.550
13751, 0.0,-1.250	20501, 0.0,-2.600
14001, 0.0,-1.300	20751, 0.0,-2.650
14251, 0.0,-1.350	21001, 0.0,-2.700
14501, 0.0,-1.400	21251, 0.0,-2.750
14751, 0.0,-1.450	21501, 0.0,-2.800
15001, 0.0,-1.500	21751, 0.0,-2.850
15251, 0.0,-1.550	22001, 0.0,-2.900
15501, 0.0,-1.600	22251, 0.0,-2.950
15751, 0.0,-1.650	22501, 0.0,-3.000
16001, 0.0,-1.700	22751, 0.0,-3.050
16251, 0.0,-1.750	23001, 0.0,-3.100
16501, 0.0,-1.800	23251, 0.0,-3.150
16751, 0.0,-1.850	23501, 0.0,-3.200
17001, 0.0,-1.900	23751, 0.0,-3.250

24001, 0.0,-3.300	30751, 0.0,-4.650
24251, 0.0,-3.350	31001, 0.0,-4.700
24501, 0.0,-3.400	31251, 0.0,-4.750
24751, 0.0,-3.450	31501, 0.0,-4.800
25001, 0.0,-3.500	31751, 0.0,-4.850
25251, 0.0,-3.550	32001, 0.0,-4.900
25501, 0.0,-3.600	32251, 0.0,-4.950
25751, 0.0,-3.650	32501, 0.0,-5.000
26001, 0.0,-3.700	32751, 0.0,-5.050
26251, 0.0,-3.750	33001, 0.0,-5.100
26501, 0.0,-3.800	33251, 0.0,-5.150
26751, 0.0,-3.850	33501, 0.0,-5.200
27001, 0.0,-3.900	33751, 0.0,-5.250
27251, 0.0,-3.950	34001, 0.0,-5.300
27501, 0.0,-4.000	34251, 0.0,-5.350
27751, 0.0,-4.050	34501, 0.0,-5.400
28001, 0.0,-4.100	34751, 0.0,-5.450
28251, 0.0,-4.150	35001, 0.0,-5.500
28501, 0.0,-4.200	35251, 0.0,-5.550
28751, 0.0,-4.250	35501, 0.0,-5.600
29001, 0.0,-4.300	35751, 0.0,-5.650
29251, 0.0,-4.350	36001, 0.0,-5.700
29501, 0.0,-4.400	36251, 0.0,-5.750
29751, 0.0,-4.450	36501, 0.0,-5.800
30001, 0.0,-4.500	36751, 0.0,-5.850
30251, 0.0,-4.550	37001, 0.0,-5.900
30501, 0.0,-4.600	37251, 0.0,-5.950

37501, 0.0,-6.000	44251, 0.0,-7.350
37751, 0.0,-6.050	44501, 0.0,-7.400
38001, 0.0,-6.100	44751, 0.0,-7.450
38251, 0.0,-6.150	45001, 0.0,-7.500
38501, 0.0,-6.200	45251, 0.0,-7.600
38751, 0.0,-6.250	45501, 0.0,-7.700
39001, 0.0,-6.300	45751, 0.0,-7.800
39251, 0.0,-6.350	46001, 0.0,-7.900
39501, 0.0,-6.400	46251, 0.0,-8.000
39751, 0.0,-6.450	46501, 0.0,-8.100
40001, 0.0,-6.500	46751, 0.0,-8.200
40251, 0.0,-6.550	47001, 0.0,-8.300
40501, 0.0,-6.600	47251, 0.0,-8.400
40751, 0.0,-6.650	47501, 0.0,-8.500
41001, 0.0,-6.700	47751, 0.0,-8.600
41251, 0.0,-6.750	48001, 0.0,-8.700
41501, 0.0,-6.800	48251, 0.0,-8.800
41751, 0.0,-6.850	48501, 0.0,-8.900
42001, 0.0,-6.900	48751, 0.0,-9.000
42251, 0.0,-6.950	49001, 0.0,-9.100
42501, 0.0,-7.000	49251, 0.0,-9.200
42751, 0.0,-7.050	49501, 0.0,-9.300
43001, 0.0,-7.100	49751, 0.0,-9.400
43251, 0.0,-7.150	50001, 0.0,-9.500
43501, 0.0,-7.200	50251, 0.0,-9.600
43751, 0.0,-7.250	50501, 0.0,-9.700
44001, 0.0,-7.300	50751, 0.0,-9.800

51001, 0.0,-9.900	57751, 0.0,-48.000
51251, 0.0,-10.000	58001, 0.0,-50.000
51501, 0.0,-10.200	58251, 0.0,-55.000
51751, 0.0,-10.500	58501, 0.0,-60.000
52001, 0.0,-11.000	58751, 0.0,-65.000
52251, 0.0,-12.000	59001, 0.0,-70.000
52501, 0.0,-13.000	59251, 0.0,-75.000
52751, 0.0,-14.000	59501, 0.0,-80.000
53001, 0.0,-15.000	59751, 0.0,-90.000
53251, 0.0,-16.000	60001, 0.0,-100.000
53501, 0.0,-17.000	60251, 0.0,-120.000
53751, 0.0,-18.000	60501, 0.0,-160.000
54001, 0.0,-19.000	60751, 0.0,-200.000
54251, 0.0,-20.000	*node, nset=right
54501, 0.0,-22.000	250, 200.0,0.000
54751, 0.0,-24.000	500, 200.0,-0.020
55001, 0.0,-26.000	750, 200.0,-0.040
55251, 0.0,-28.000	1000, 200.0,-0.060
55501, 0.0,-30.000	1250, 200.0,-0.080
55751, 0.0,-32.000	1500, 200.0,-0.100
56001, 0.0,-34.000	1750, 200.0,-0.120
56251, 0.0,-36.000	2000, 200.0,-0.140
56501, 0.0,-38.000	2250, 200.0,-0.160
56751, 0.0,-40.000	2500, 200.0,-0.180
57001, 0.0,-42.000	2750, 200.0,-0.200
57251, 0.0,-44.000	3000, 200.0,-0.220
57501, 0.0,-46.000	3250, 200.0,-0.240

3500, 200.0,-0.260	10250, 200.0,-0.800
3750, 200.0,-0.280	10500, 200.0,-0.820
4000, 200.0,-0.300	10750, 200.0,-0.840
4250, 200.0,-0.320	11000, 200.0,-0.860
4500, 200.0,-0.340	11250, 200.0,-0.880
4750, 200.0,-0.360	11500, 200.0,-0.900
5000, 200.0,-0.380	11750, 200.0,-0.920
5250, 200.0,-0.400	12000, 200.0,-0.940
5500, 200.0,-0.420	12250, 200.0,-0.960
5750, 200.0,-0.440	12500, 200.0,-0.980
6000, 200.0,-0.460	12750, 200.0,-1.000
6250, 200.0,-0.480	13000, 200.0,-1.050
6500, 200.0,-0.500	13250, 200.0,-1.100
6750, 200.0,-0.520	13500, 200.0,-1.150
7000, 200.0,-0.540	13750, 200.0,-1.200
7250, 200.0,-0.560	14000, 200.0,-1.250
7500, 200.0,-0.580	14250, 200.0,-1.300
7750, 200.0,-0.600	14500, 200.0,-1.350
8000, 200.0,-0.620	14750, 200.0,-1.400
8250, 200.0,-0.640	15000, 200.0,-1.450
8500, 200.0,-0.660	15250, 200.0,-1.500
8750, 200.0,-0.680	15500, 200.0,-1.550
9000, 200.0,-0.700	15750, 200.0,-1.600
9250, 200.0,-0.720	16000, 200.0,-1.650
9500, 200.0,-0.740	16250, 200.0,-1.700
9750, 200.0,-0.760	16500, 200.0,-1.750
10000, 200.0,-0.780	16750, 200.0,-1.800

17000, 200.0,-1.850	23750, 200.0,-3.200
17250, 200.0,-1.900	24000, 200.0,-3.250
17500, 200.0,-1.950	24250, 200.0,-3.300
17750, 200.0,-2.000	24500, 200.0,-3.350
18000, 200.0,-2.050	24750, 200.0,-3.400
18250, 200.0,-2.100	25000, 200.0,-3.450
18500, 200.0,-2.150	25250, 200.0,-3.500
18750, 200.0,-2.200	25500, 200.0,-3.550
19000, 200.0,-2.250	25750, 200.0,-3.600
19250, 200.0,-2.300	26000, 200.0,-3.650
19500, 200.0,-2.350	26250, 200.0,-3.700
19750, 200.0,-2.400	26500, 200.0,-3.750
20000, 200.0,-2.450	26750, 200.0,-3.800
20250, 200.0,-2.500	27000, 200.0,-3.850
20500, 200.0,-2.550	27250, 200.0,-3.900
20750, 200.0,-2.600	27500, 200.0,-3.950
21000, 200.0,-2.650	27750, 200.0,-4.000
21250, 200.0,-2.700	28000, 200.0,-4.050
21500, 200.0,-2.750	28250, 200.0,-4.100
21750, 200.0,-2.800	28500, 200.0,-4.150
22000, 200.0,-2.850	28750, 200.0,-4.200
22250, 200.0,-2.900	29000, 200.0,-4.250
22500, 200.0,-2.950	29250, 200.0,-4.300
22750, 200.0,-3.000	29500, 200.0,-4.350
23000, 200.0,-3.050	29750, 200.0,-4.400
23250, 200.0,-3.100	30000, 200.0,-4.450
23500, 200.0,-3.150	30250, 200.0,-4.500

30500, 200.0,-4.550	37250, 200.0,-5.900
30750, 200.0,-4.600	37500, 200.0,-5.950
31000, 200.0,-4.650	37750, 200.0,-6.000
31250, 200.0,-4.700	38000, 200.0,-6.050
31500, 200.0,-4.750	38250, 200.0,-6.100
31750, 200.0,-4.800	38500, 200.0,-6.150
32000, 200.0,-4.850	38750, 200.0,-6.200
32250, 200.0,-4.900	39000, 200.0,-6.250
32500, 200.0,-4.950	39250, 200.0,-6.300
32750, 200.0,-5.000	39500, 200.0,-6.350
33000, 200.0,-5.050	39750, 200.0,-6.400
33250, 200.0,-5.100	40000, 200.0,-6.450
33500, 200.0,-5.150	40250, 200.0,-6.500
33750, 200.0,-5.200	40500, 200.0,-6.550
34000, 200.0,-5.250	40750, 200.0,-6.600
34250, 200.0,-5.300	41000, 200.0,-6.650
34500, 200.0,-5.350	41250, 200.0,-6.700
34750, 200.0,-5.400	41500, 200.0,-6.750
35000, 200.0,-5.450	41750, 200.0,-6.800
35250, 200.0,-5.500	42000, 200.0,-6.850
35500, 200.0,-5.550	42250, 200.0,-6.900
35750, 200.0,-5.600	42500, 200.0,-6.950
36000, 200.0,-5.650	42750, 200.0,-7.000
36250, 200.0,-5.700	43000, 200.0,-7.050
36500, 200.0,-5.750	43250, 200.0,-7.100
36750, 200.0,-5.800	43500, 200.0,-7.150
37000, 200.0,-5.850	43750, 200.0,-7.200

44000, 200.0,-7.250	50750, 200.0,-9.700
44250, 200.0,-7.300	51000, 200.0,-9.800
44500, 200.0,-7.350	51250, 200.0,-9.900
44750, 200.0,-7.400	51500, 200.0,-10.000
45000, 200.0,-7.450	51750, 200.0,-10.200
45250, 200.0,-7.500	52000, 200.0,-10.500
45500, 200.0,-7.600	52250, 200.0,-11.000
45750, 200.0,-7.700	52500, 200.0,-12.000
46000, 200.0,-7.800	52750, 200.0,-13.000
46250, 200.0,-7.900	53000, 200.0,-14.000
46500, 200.0,-8.000	53250, 200.0,-15.000
46750, 200.0,-8.100	53500, 200.0,-16.000
47000, 200.0,-8.200	53750, 200.0,-17.000
47250, 200.0,-8.300	54000, 200.0,-18.000
47500, 200.0,-8.400	54250, 200.0,-19.000
47750, 200.0,-8.500	54500, 200.0,-20.000
48000, 200.0,-8.600	54750, 200.0,-22.000
48250, 200.0,-8.700	55000, 200.0,-24.000
48500, 200.0,-8.800	55250, 200.0,-26.000
48750, 200.0,-8.900	55500, 200.0,-28.000
49000, 200.0,-9.000	55750, 200.0,-30.000
49250, 200.0,-9.100	56000, 200.0,-32.000
49500, 200.0,-9.200	56250, 200.0,-34.000
49750, 200.0,-9.300	56500, 200.0,-36.000
50000, 200.0,-9.400	56750, 200.0,-38.000
50250, 200.0,-9.500	57000, 200.0,-40.000
50500, 200.0,-9.600	57250, 200.0,-42.000

57500, 200.0,-44.000	1141063,	0.0,	0.006
57750, 200.0,-46.000	1141094,	0.0,	0.009
58000, 200.0,-48.000	1141125,	0.0,	0.015
58250, 200.0,-50.000	1141156,	0.0,	0.021
58500, 200.0,-55.000	1141187,	0.0,	0.027
58750, 200.0,-60.000	1141218,	0.0,	0.036
59000, 200.0,-65.000	1141249,	0.0,	0.045
59250, 200.0,-70.000	1141280,	0.0,	0.054
59500, 200.0,-75.000	1141311,	0.0,	0.063
59750, 200.0,-80.000	1141342,	0.0,	0.075
60000, 200.0,-90.000	1141373,	0.0,	0.087
60250, 200.0,-100.000	1141404,	0.0,	0.099
60500, 200.0,-120.000	1141435,	0.0,	0.111
60750, 200.0,-160.000	1141466,	0.0,	0.123
61000, 200.0,-200.000	1141497,	0.0,	0.141
*nset, nset=bottom, generate	1141528,	0.0,	0.165
60751, 61000, 1	1141559,	0.0,	0.18
*nset, nset=top, generate	1141590,	0.0,	0.24
1, 250, 1	1141621,	0.0,	0.3
** "normal" bias: 0.973, use 0.97 to test shallow indentation	1141652,	0.0,	0.45
*nfill, bias=0.976	1141683,	0.0,	0.6
left, right, 249, 1	1141714,	0.0,	0.75
**	1141745,	0.0,	0.9
** indenter nodes	1141776,	0.0,	1.05
*node, nset=ind-left	1141807,	0.0,	1.2
1141001, 0.0, 0.0003	1141838,	0.0,	1.35
1141032, 0.0, 0.003	1141869,	0.0,	4

1141900,	0.0,	9	1141775,	18.0,	7.5
1141931,	0.0,	14	1141806,	18.0,	7.6
*node, nset=ind-righ			1141837,	18.0,	7.7
1141031,	18.0,	6.45	1141868,	18.0,	7.8
1141062,	18.0,	6.451	1141899,	18.0,	7.9
1141093,	18.0,	6.452	1141930,	18.0,	10
1141124,	18.0,	6.453	1141961,	18.0,	14
1141155,	18.0,	6.454	*nfill, bias=0.84		
1141186,	18.0,	6.455	ind-left, ind-right, 30, 1		
1141217,	18.0,	6.456	*nset, nset=ind-all, generate		
1141248,	18.0,	6.457	1141001, 1141961, 1		
1141279,	18.0,	6.458	*nset, nset=ind-top, generate		
1141310,	18.0,	6.459	1141931, 1141961, 1		
1141341,	18.0,	6.46	*nset, nset=ind-bot, generate		
1141372,	18.0,	6.461	1141001, 1141031, 1		
1141403,	18.0,	6.462	*nset, nset=ind-tip		
1141434,	18.0,	6.463	1141961		
1141465,	18.0,	6.563	*nset, nset=indtop-1, generate		
1141496,	18.0,	6.663	1141931, 1141960, 1		
1141527,	18.0,	6.763	*nset, nset=All, generate		
1141558,	18.0,	6.863	1,180000,1,		
1141589,	18.0,	6.963	**		
1141620,	18.0,	7	**		
1141651,	18.0,	7.1	**ELEMENT INFORMATION		
1141682,	18.0,	7.2	**		
1141713,	18.0,	7.3	*Element, type=CAX4		
1141744,	18.0,	7.4	1, 251, 252, 2, 1		

```

*elgen, elset=whole
1, 249, 1, 1, 243, 250, 249
**elset, elset=film, generate
**1, 11940, 1
*elset, elset=up_film, generate
1, 700, 1
*elset, elset=low_film, generate
701,42330, 1
*elset, elset=sub, generate
42331, 60507, 1
**
*Elset, elset=Set-1, generate
1, 200, 1
**
*Elset, elset=__PickedSurf7_S3,
generate
1, 200, 1
**
*element, type=cax4
1141001, 1141001, 1141002, 1141033,
1141032
*elgen, elset=indenter
1141001, 30, 1, 1, 30, 31, 30
*elset, elset=ind_bot_ele, generate
1141001, 1141030, 1
**
*surface, name=indsurf
ind_bot_ele, s1
**
**Surface, name=_PickedSurf7
__PickedSurf7_S3, S3
*Contact Pair, interaction=IntProp-1
_PickedSurf7, indsurf
*Surface Interaction, name=IntProp-1
*Friction
0.1
**
*solid section, elset=up_film,
material=sn
*solid section, elset=low_film,
material=sn
*solid section, elset=sub, material=sn
*Solid Section, elset=indenter,
material=diamond
**
*material, name=diamond
*elastic
1141000.0, 0.07
**
*MATERIAL, NAME=sn
*ELASTIC
46000.0, 0.34
*Plastic
1.9,0.0
**10.0,0.3
*rate dependent,type=yield ratio

```

```

1.0, 0.0
1.0, 1.107e-10
1.05, 1.585e-10
1.11, 2.230e-10
2.11, 2.028e-8
3.16, 3.46e-7
4.21, 2.597e-6
4.73, 5.922e-6
5.79, 2.413e-5
7.37, 1.31e-4
**
**
**BOUNDARY CONDITIONS
**EQUATION
2
indtop-1, 2, 1.0, 1141961, 2, -1.0
**
*Boundary
Left, 1
Bottom, 2
ind-left, 1
**
**
*RESTART,WRITE,OVERLAY
** -----
-----
**
** STEP: Step-1
**
**
**
loading
*static
0.05, 10000, 0.0005, 10000
**
*CONTROLS,
ANALYSIS=DISCONTINUOUS
*CONTROLS, PARAMETERS=LINE
SEARCH
4,4,0.25,0.25,0.15
** BOUNDARY CONDITIONS
**
*Boundary
ind-tip, 2, 2, -.4
**
** OUTPUT REQUESTS
*OUTPUT,FIELD,FREQUENCY=100
*NODE OUTPUT
U,RF
*NODE OUTPUT, NSET=top
COORD
*ELEMENT OUTPUT
S,MISES,E,PEEQ,EE
*CONTACT
OUTPUT,VARIABLE=PRESELECT,N
SET=top
*NODE print,NSET=ind-
tip,frequency=1

```



```

U,RF2
*node print, nset=top,frequency=50000
coord, U, RF2
*OUTPUT,FIELD,variables=preselect
*OUTPUT,HISTORY,variables=preselect, frequency=1
*NODE OUTPUT,NSET=ind-tip
u2, rf2
*node output, nset=top
U
*End Step
** STEP: Step-2
**
*Step, INC=600000, NLGEOM=YES,
UNSYMM=YES
loading
*static
0.05, 5000, 0.0005, 5000
**
*CONTROLS,
ANALYSIS=DISCONTINUOUS
*CONTROLS, PARAMETERS=LINE
SEARCH
4,4,0.25,0.25,0.15
** BOUNDARY CONDITIONS
**
*Boundary
ind-tip, 2, 2, -.8
**

```

```

** OUTPUT REQUESTS
*OUTPUT,FIELD,FREQUENCY=100
*NODE OUTPUT
U,RF
*NODE OUTPUT, NSET=top
COORD
*ELEMENT OUTPUT
S,MISES,E,PEEQ,EE
*CONTACT
OUTPUT,VARIABLE=PRESELECT,N
SET=top
*NODE print,NSET=ind-
tip,frequency=1
U,RF2
*node print, nset=top,frequency=50000
coord, U, RF2
*OUTPUT,FIELD,variables=preselect
*OUTPUT,HISTORY,variables=preselect, frequency=1
*NODE OUTPUT,NSET=ind-tip
u2, rf2
*node output, nset=top
U
*End Step
** STEP: Step-3
**
*Step, INC=600000, NLGEOM=YES,
UNSYMM=YES
*static

```

```

0.05, 3333.3,0.0005,3333.3
**
*CONTROLS,
ANALYSIS=DISCONTINUOUS
**
*CONTROLS, PARAMETERS=LINE
SEARCH
4,4,0.25,0.25,0.15
** BOUNDARY CONDITIONS
**
*Boundary
ind-tip, 2, 2, -1.2
**
** OUTPUT REQUESTS
*OUTPUT,FIELD,FREQUENCY=100
*NODE OUTPUT
U,RF
**
*NODE OUTPUT, NSET=top
COORD
**
*ELEMENT OUTPUT
S,MISES,E,PEEQ,EE
**
*CONTACT
OUTPUT,VARIABLE=PRESELECT,N
SET=top
**
*NODE print,NSET=ind-
tip,frequency=1
U,RF2
**
*node print, nset=top,frequency=500000
coord, U, RF2
**
*OUTPUT,FIELD,variables=preselect
*OUTPUT,HISTORY,variables=presele
ct, frequency=1
**
*NODE OUTPUT,NSET=ind-tip
u2, rf2
**
*node output, nset=top
U
**
*End Step
**
** STEP: Step-4
**
*Step, INC=600000, NLGEOM=YES,
UNSYMM=YES
loading
**
*static
0.05, 2500, 0.0005, 2500
**
*CONTROLS,
ANALYSIS=DISCONTINUOUS
**
*CONTROLS, PARAMETERS=LINE
SEARCH
4,4,0.25,0.25,0.15
** BOUNDARY CONDITIONS
**
*Boundary
ind-tip, 2, 2, -1.6
**
** OUTPUT REQUESTS
*OUTPUT,FIELD,FREQUENCY=100
*NODE OUTPUT

```

U,RF
 *NODE OUTPUT, NSET=top
 COORD
 *ELEMENT OUTPUT
 S,MISES,E,PEEQ,EE
 *CONTACT
 OUTPUT, VARIABLE=PRESELECT,N
 SET=top
 *NODE print,NSET=ind-
 tip,frequency=1
 U,RF2
 *node print, nset=top,frequency=50000
 coord, U, RF2
 *OUTPUT,FIELD,variables=preselect
 *OUTPUT,HISTORY,variables=preselect,
 frequency=1
 *NODE OUTPUT,NSET=ind-tip
 u2, rf2
 *node output, nset=top
 U
 *End Step
 ** STEP: Step-5
 **
 *Step, INC=600000, NLGEOM=YES,
 UNSYMM=YES
 loading
 *static
 0.5, 2000, 0.005, 2000
 **

*CONTROLS,
 ANALYSIS=DISCONTINUOUS
 *CONTROLS, PARAMETERS=LINE
 SEARCH
 4,4,0.25,0.25,0.15
 ** BOUNDARY CONDITIONS
 **
 *Boundary
 ind-tip, 2, 2, -2.0
 **
 ** OUTPUT REQUESTS
 *OUTPUT,FIELD,FREQUENCY=1000
 *NODE OUTPUT
 U,RF
 *NODE OUTPUT, NSET=top
 COORD
 *ELEMENT OUTPUT
 S,MISES,E,PEEQ,EE
 *CONTACT
 OUTPUT, VARIABLE=PRESELECT,N
 SET=top
 *NODE print,NSET=ind-
 tip,frequency=1
 U,RF2
 *node print, nset=top,frequency=50000
 coord, U, RF2
 *OUTPUT,FIELD,variables=preselect
 *OUTPUT,HISTORY,variables=preselect,
 frequency=1
 *NODE OUTPUT,NSET=ind-tip

```

u2, rf2
*node output, nset=top
U
*End Step
** STEP: Step-6
**
*Step, INC=600000, NLGEOM=YES,
UNSYMM=YES
loading
*static
0.5, 1666.6,0.005, 1666.6
**
*CONTROLS,
ANALYSIS=DISCONTINUOUS
*CONTROLS, PARAMETERS=LINE
SEARCH
4,4,0.25,0.25,0.15
** BOUNDARY CONDITIONS
**
*Boundary
ind-tip, 2, 2, -2.4
**
** OUTPUT REQUESTS
*OUTPUT,FIELD,FREQUENCY=1000
*NODE OUTPUT
U,RF
*NODE OUTPUT, NSET=top
COORD

```

```

*ELEMENT OUTPUT
S,MISES,E,PEEQ,EE
*CONTACT
OUTPUT,VARIABLE=PRESELECT,N
SET=top
*NODE print,NSET=ind-
tip,frequency=1
U,RF2
*node print, nset=top,frequency=50000
coord, U, RF2
*OUTPUT,FIELD,variables=preselect
*OUTPUT,HISTORY,variables=presele
ct, frequency=1
*NODE OUTPUT,NSET=ind-tip
u2, rf2
*node output, nset=top
U
*End Step
**
** STEP: Step-7
**
*Step, INC=600000, NLGEOM=YES,
UNSYMM=YES
loading
*static
0.5, 1428.5, 0.005, 1428.5
**
*CONTROLS,
ANALYSIS=DISCONTINUOUS

```

```

*CONTROLS, PARAMETERS=LINE SEARCH
4,4,0.25,0.25,0.15
** BOUNDARY CONDITIONS
**
*Boundary
ind-tip, 2, 2, -2.8
**
** OUTPUT REQUESTS
*OUTPUT,FIELD,FREQUENCY=1000
*NODE OUTPUT
U,RF
*NODE OUTPUT, NSET=top
COORD
*ELEMENT OUTPUT
S,MISES,E,PEEQ,EE
*CONTACT
OUTPUT,VARIABLE=PRESELECT,N
SET=top
*NODE print,NSET=ind-
tip,frequency=1
U,RF2
*node print, nset=top,frequency=50000
coord, U, RF2
*OUTPUT,FIELD,variables=preselect
*OUTPUT,HISTORY,variables=preselect,
frequency=1
*NODE OUTPUT,NSET=ind-tip
u2, rf2

*node output, nset=top
U
*End Step
**
** STEP: Step-8
**
*Step, INC=600000, NLGEOM=YES,
UNSYMM=YES
loading
*static
0.5, 1250, 0.005, 1250
**
*CONTROLS,
ANALYSIS=DISCONTINUOUS
*CONTROLS, PARAMETERS=LINE SEARCH
4,4,0.25,0.25,0.15
** BOUNDARY CONDITIONS
**
*Boundary
ind-tip, 2, 2, -3.2
**
** OUTPUT REQUESTS
*OUTPUT,FIELD,FREQUENCY=1000
*NODE OUTPUT
U,RF
*NODE OUTPUT, NSET=top
COORD

```

*ELEMENT OUTPUT	4,4,0.25,0.25,0.15
S,MISES,E,PEEQ,EE	** BOUNDARY CONDITIONS
*CONTACT	**
OUTPUT,VARIABLE=PRESELECT,N	*Boundary
SET=top	ind-tip, 2, 2,-3.6
*NODE print,NSET=ind-	**
tip,frequency=1	** OUTPUT REQUESTS
U,RF2	*OUTPUT,FIELD,FREQUENCY=1000
*node print, nset=top,frequency=50000	*NODE OUTPUT
coord, U, RF2	U,RF
*OUTPUT,FIELD,variables=preselect	*NODE OUTPUT, NSET=top
*OUTPUT,HISTORY,variables=preselect,	COORD
frequency=1	*ELEMENT OUTPUT
*NODE OUTPUT,NSET=ind-tip	S,MISES,E,PEEQ,EE
u2, rf2	*CONTACT
*node output, nset=top	OUTPUT,VARIABLE=PRESELECT,N
U	SET=top
*End Step	*NODE print,NSET=ind-
**** STEP: Step-9	tip,frequency=1
**	U,RF2
*Step, INC=600000, NLGEOM=YES,	*node print, nset=top,frequency=50000
UNSYMM=YES	coord, U, RF2
loading	*OUTPUT,FIELD,variables=preselect
*static	*OUTPUT,HISTORY,variables=preselect,
1.0, 1111.1, 0.05, 1111.1	frequency=1
**	*NODE OUTPUT,NSET=ind-tip
*CONTROLS,	u2, rf2
ANALYSIS=DISCONTINUOUS	*node output, nset=top
*CONTROLS, PARAMETERS=LINE	U
SEARCH	

```

*End Step
**** STEP: Step-10
**
*Step, INC=600000, NLGEOM=YES,
UNSYMM=YES
loading
*static
1.0, 1000, 0.05, 1000
**
*CONTROLS,
ANALYSIS=DISCONTINUOUS
*CONTROLS, PARAMETERS=LINE
SEARCH
4,4,0.25,0.25,0.15
** BOUNDARY CONDITIONS
**
*Boundary
ind-tip, 2, 2, -4.0
**
** OUTPUT REQUESTS
*OUTPUT,FIELD,FREQUENCY=1000
*NODE OUTPUT
U,RF
*NODE OUTPUT, NSET=top
COORD
*ELEMENT OUTPUT
S,MISES,E,PEEQ,EE
*CONTACT
OUTPUT,VARIABLE=PRESELECT,N
SET=top
*NODE print,NSET=ind-
tip,frequency=1
U,RF2
*node print, nset=top,frequency=50000
coord, U, RF2
*OUTPUT,FIELD,variables=preselect
*OUTPUT,HISTORY,variables=presele
ct, frequency=1
*NODE OUTPUT,NSET=ind-tip
u2, rf2
*node output, nset=top
U
*End Step
**
**** STEP: Step-11
**
*Step, INC=600000, NLGEOM=YES,
UNSYMM=YES
loading
*static
0.05, 16.0, 0.0005, 16
**
*CONTROLS,
ANALYSIS=DISCONTINUOUS
*CONTROLS, PARAMETERS=LINE
SEARCH
4,4,0.25,0.25,0.15

```

```

** BOUNDARY CONDITIONS **
**
*Boundary
ind-tip, 2, 2, 0
**
** OUTPUT REQUESTS
*OUTPUT,FIELD,FREQUENCY=1000
*NODE OUTPUT
U,RF
*NODE OUTPUT, NSET=top
COORD
*ELEMENT OUTPUT
S,MISES,E,PEEQ,EE
*CONTACT
OUTPUT, VARIABLE=PRESELECT,N
SET=top
*NODE print,NSET=ind-
tip,frequency=1
U,RF2
*node print, nset=top,frequency=50000
coord, U, RF2
*OUTPUT,FIELD,variables=preselect
*OUTPUT,HISTORY,variables=preselect,
frequency=1
*NODE OUTPUT,NSET=ind-tip
u2, rf2
*node output, nset=top
U
*End Step

```